

Geologically, the simulation area is underlain by Pre-Tertiary shales, Tertiary volcanic to intrusive rocks, and Quaternary terrace deposits. Pre-Tertiary and Tertiary rocks are usually compact and not permeable except around fissures along the Magistral river and terrace deposits.

As the results of the electrical prospecting and boring observation, low resistivity zone and low-high complex resistivity zone correspond to aquifer. Intermediate resistivity zone corresponds to aquitard. High resistivity zone corresponds to aquiclude and aquifuge.

As compared with geology and geological structure, The aquifer zone is equivalent to the boundary between sandy terrace deposit and lower formations, fault zone, intrusive rocks periphery. The aquitard is equivalent to weathered overburden and fault periphery. The aquiclude is equivalent to surface soil and calyey terrace deposit. The aquifuge is equivalent to the compact Pre-tertiary, Tertiary and intrusive rocks on the mountain to hill sides.

As the results (Table 5-4-7) of grain size distribution, the aquiclude permeability coefficient of Recent terrace deposits ranges 10^{-5} to 10^{-7} cm/sec (CR-1,2). That of Pleistocene terrace deposits ranges 10^{-5} to 10^{-7} cm/sec (CR-3,4,5,6). The soil test for new tailing dam indicates $10^{-4} \sim 10^{-5}$ cm/sec as to aquiclude clayey terrace deposits (D-1 to D-10), and 10^{-3} cm/sec as to aquifer sandy terrace deposits (B-11,12), as Table 5-6-2 shows. Consequently, the aquifer and aquiclude permeability coefficients are set to 10^{-3} cm/sec and 10^{-5} cm/sec on the average, respectively. The other permeability coefficient values are given in the same way as the Parral area.

Along the Magistral river, several faults are developed in the pre-Tertiary and Tertiary rocks. Permeability coefficient of these fractures is different from its peripheral rocks. this permeability coefficient of these fractures is named fracture permeability coefficient (pkf). To the contrary, the permeability coefficient of the peripheral rocks is named matrix permeability coefficient (pkm). From this basis, The average permeability coefficient (K) of the simulation block is calculated as follows.

$$K = (h_{ef} / \Delta X) \times pkf + (1 - h_{ef} / \Delta X) \times pkm$$

ΔX : width of fracture

h_{ef} : width of block

The porosity is also distinguished fracture porosity (porf) from matrix

porosity (porm) and is given the value corresponds to the hydraulic observation.

Table 5-4-8 shows the permeability coefficient and porosity model, and Fig.5-4-10 shows the rock classification maps on the basis of this concept.

In this Fig.5-4-10 plane map (X-Y CROSS SECTIONAL VIEW), the coordinates of left-bottom and right-top ends are (X1,Y1) and (X25,Y29), respectively. In the cross section (Y-Z CROSS SECTIONAL VIEW), left and right ends are Y29 and Y1, respectively. The legend No. of Table 5-4-8 corresponds to it of Fig.5-4-10.

③ Hydraulic Model

As Fig.5-4-1 shows, No.1 river flow measuring point is situated upstream of the Magistral river. In the dry season, at this point, flow rate is $415 \text{ m}^3/\text{day}$. At No.2 point dwonstream of the magistral river, flow rate is $0 \text{ m}^3/\text{sec}$ because of infiltration. In tributary of this river, the water flow is not observed. On the other hand, in the rainy season, the continuous waterflow is recognized in the Magistral river. No.1 point flow rate is $4,000$ to $86,000 \text{ m}^3/\text{day}$, No.2 point flow rate is $7,000$ to $28,000 \text{ m}^3/\text{day}$ as Fig.5-4-2 shows.

In both seasons, at No.2 point, the river flow reduces because of infiltration between No.1 and No.2 point. The large faults are observed along these points, and control the infiltration of riverwater, so that initial river flows are set as $415 \text{ m}^3/\text{day}$ in dry season during November to May and $4,000 \text{ m}^3/\text{day}$ in the rainy season at No.1 point, respectively. The tributary streams don not have initial river flow, because of non flow observation in both seasons.

Each water level of the observation wells is set for simulation as to be situated at the top of the third layer counted from atmosphere layer. Though the boring B-2 is flowing well at the rate of $120 \text{ m}^3/\text{day}$, the water level is set at the top of the third layer which is uppermost of Tertiary rock, because the water level was set at this depth before boring.

④ Meteorological Model

Annual precipitation is 800 mm on the average during 1985 to 1990. 90 percent of it precipitate during rainy season from June to October. Therefore, during these 5 months, the precipitation is 720 mm from June to October. During other 7 months the precipitation is 80 mm .

Evaporation data are referred from New El Coco observation. Evaporation of

it ranges 0.35 to 0.84mm/day.

Recharge rate is set as 0mm/day during the dry season, 4mm/day during the rainy season, by precipitation minus evaporation.

⑤ Tailing Dam Model

A new tailing dam is planned to set up on the terrace deposits along the old path of Magistral river as Fig.5-4-9 shows.

To estimate the influence to the surroundings by the construction of a new tailing dam, Another simulation is carried out under the condition of including the dam data which are consist of scale, permeability, porosity, recharge, and discharge models.

As described in the Paragraph 5-6, the planned dam is 300m long, 100 wide, 10m thick, and $3 \times 10^5 \text{m}^3$ volume. In this simulation after constructing a tailing dam, the simulation blocks of the dam is set in this site. The permeability of the tailings is adapted it from El Bote and Parral tailings, that is 10^{-8}cm/sec . The block model is shown in Fig.5-4-13, and the dam site is situated at the D site on the map.

⑥ Recharge and Discharge Model

Waste water discharged is set as $200 \text{m}^3/\text{day}$, as tailings discharge is estimated as $200/\text{day}$. $50 \text{m}^3/\text{day}$ out of $200 \text{m}^3/\text{day}$ waste water is recycled by being stored in the deposition pond, which is used to prevent the surface runoff of the waste water. $150 \text{m}^3/\text{day}$ groundwater is pumped up from two boring holes, which is 25m short with full strainer. The boring sites are shown in Fig.5-4-9. The main pumping depth is set in the fifth layer for simulation.

The water for living supply is planned to be used from boring well B-2, from which groundwater discharged at the rate of $120 \text{m}^3/\text{day}$. This water is set to be directly discharged to the river near the pond. this site is situated at the top of the third layer.

(3) Simulation Results (before Constructing a Tailing Dam)

Fig.5-4-11 shows groundwater saturation map before constructing a tailing dam. Rainy season map is of the 150th day, counted from the first day of rainy season. Dry season map is the 360th day, counted from the first day of rainy

season. In this maps, blue color is 100% saturated with free water. In accordance with the changing blue to yellow, the saturation level decreases.

The groundwater is recognized below than the second layer at the bore hole B-2 and upstream. But, the water level is drawn down downstream. This appearance corresponds to the reduction between No.1 and No.2 site in Fig.5-4-1,2, that is, infiltration of riverwater.

The water table is continued to it of the Magistral river below the fourth layer. Saturation level is lower in the surface layer in the dry season than that in the rainy season. In the dry season, Unsaturated area widens around saturated area ,and this unsaturation leads to the drawdown. But, this drawdown is not remarkable among in the dry and rainy seasons ,and corresponds to the field observation of bore hole water level.

Fig.5-4-12 shows groundwater velocity plane and cross sectional map. The rainy season map is of the 150th day, and the dry season map is of the 360th day, counted from the first day from the rainy season, respectively .

The velocity is presented by X, Y, and Z components, i.e. NW-SE, NE-SW, and vertical direction, respectively. The length of arrow is in proportion to the groundwater flow velocity.

The fourth layers plane map of the rainy season indicates clear northwestern flow directions ,which runs to the Magistral river, around the dam site (site A on the map) ,and northern terrace deposits area (site B). This flow changes in the southwest direction around the Magistral river. This tendency is not different in the dry season, but the velocity is slightly low.

The cross sectional velocity maps show down-flow in the surface layers around the dam site (site A) and northern terrace deposits site (site B). In the deep layers, The lateral flow from site B to site A is obvious. this direction is not changeable during the rainy and dry seasons , but velocity is lower in the dry season in the surface layers.

(4) Simulation Results (after Constructing a Tailing Dam)

Groundwater existence below the new planned tailing dam site is clear, and this groundwater flows to the Magistral river. The hydraulic properties, obtained from this simulation, should be applied to model the dam construction.

The shape and volume of the Tailing dam is described in Paragraph 4-6.

The model of two pumping bore holes, one deposition pond, and other facilities is described in Article ⑤ Tailing Dam Model.

Fig.5-4-14 shows groundwater saturation map after constructing a tailing dam.

In the rainy season, the saturation level is slightly higher in the fourth layer around two boring sites (P1, P2 on the map), because of gathering of the water from the surrounding layers. In the dry season, more saturated zone is clarified above the fourth layer around boring site because of collecting of the groundwater.

The cross sectional velocity maps Fig.5-4-15, after constructing a tailing dam, show down-flow in the surface layers down to the sixth layer around the dam site (site D on the map). This section runs Y7 blocks and is parallel to X axis of the northwest direction. This down-flow changes to the lateral flow in the seventh and eighth layer. This lateral flow changes to up-flow around the boring site P-1 in the surface layers. The influence of pumping is not recognized in the ninth and tenth deep layers.

Even though the down-flow velocity is larger in the rainy season because of rainfall, compared with in the dry season, the boring holes recycle the waste water efficiently.

It could be thought that the polluted groundwater infiltrates to deep zone by construction of network of pipe and water paths caused by the downwards flow of groundwater under the tailing dam.

We should have a counterplan that installing some wells in the tailing dam (strainer underlie the original surface) and some deep zone wells at the neighborhood of the pumping up well.

5-5 Soil

5-5-1 Assay results

Fig.5-5-1 shows the soil sampling map at and around the proposed tailing dam site in New El Coco area. Samples, CS-A1, Cs-A2 and CS-A3, represent the dam construction site. The assay results of 7 samples are given in Table 5-5-1. In this Table, is also shown an average or standard chemical components of soil by Rose, A. T.(1979) for reference. Fig. 5-5-2 shows the areal distribution map of each element.

(1) Cu: The highest is 34 ppm of sample CS-1, while the lowest is 5 ppm of CS-A1. Average value around the dam construction site counts 18 ppm, which is close to the background value (Table 5-5-1) of 15 ppm. Samples, CS-1, CS-2 and CS-3 taken at the riverside, contain around 30 ppm.

(2) Pb: The highest is 130 ppm of samples CS-1, while the lowest 22 ppm of CS-A1. The average value around the damsite is 54 ppm, which is about three times as high as the background of 17 ppm.

(3) Zn: The highest is 190 ppm of CS-3 and the lowest is 17 ppm of CS-A1. The average around the damsite is 76 ppm, about twice as high as the background of 36 ppm.

(4) Fe: The highest is 5.4 % of CS-2 and the lowest is 0.8 % of CS-A1. The average around the dam is 2.9 %, almost equal to the background, 2.2 %.

(5) Cd: The highest is 4.9 ppm of CS-A3 and the lowest is 0.8 ppm of CS-A1. The average around the dam is 2.7 ppm, about five times as high as the background of 0.5 ppm.

(6) Sb: The highest is 81 ppm of CS-1 and the lowest is 18 ppm of CS-A1. The average around the dam is 54 ppm, about 21 times as high as the background of 2 ppm.

(7) Cr: The highest is 33 ppm of CS-2 and the lowest is 6 ppm of CS-A1. The average around the dam is 20 ppm, about half of the background, 43ppm.

(8) As: The highest is 110 ppm of CS-3 and the lowest is 4 ppm of CS-A1. The average around the dam is 44 ppm, about five times as high as the background of 8 ppm.

(9) Hg: The highest is 0.28 ppm of CS-3 and the lowest is 0.06 ppm of CS-1. The average around the dam is 0.16 ppm, about twice as high as the background of 0.06 ppm.

5-5-2 Results and Discussion

Concentration levels of the heavy metal elements in the soil of this area are almost close to those of standard soil, except Sb. In the samples taken at the riverside some elements show the higher levels than normal. This may be brought by erosion action of the river, which accompanies precipitation of certain minerals, as well as movement and reprecipitation of metals by any chemical reaction at the surface of river deposits.

One characteristic in this area is Sb concentration of 54 ppm, which is remarkably higher than the background average of 2 ppm.

5-6 Tailing Dam

Field survey was carried out in order to make further study of a model of tailing dam described in the Progress report.

The survey items were as follows;

- (1) Drilling test of foundation ground of the tailing dam
- (2) Soil property tests of foundation ground
- (3) Water level observation (Observation of phreatic surface)
- (4) Surface survey and levelling
- (5) Collection of meteorological data

5-6-1 Results of the survey

(1) Drilling test of foundation ground

As Fig.5-6-1 shows, drilling test was carried out at two points, B-11 and B-12, about 100 m west of the former drilling point, that locates on the cross section of the tailing dam. As the result of the test, detoritus with 4 ~ 7 m thick on talus deposits with about 5 ~ 10 m on the basement was observed, It was approximately the same result of the former survey. The upper layer (detoritus) mainly consists of sand and gravel. The N value is over 50 at B-11 point and average value is 40 at B-12, which show good condensation. The lower layer (river deposit) mainly consists of gravel.

(2) Sampling and laboratory soil tests

① Laboratory soil tests was carried out concerning the undisturbed samples of foundation ground of the tailing dam. They were sampled with double tube

sampler at B-11 and B-12 holes. The number of the samples, on which the test was carried out, are shown in Table 5-6-1.

② 8 items of laboratory soil test were carried out at El Bote and Parral.

③ Summary of laboratory soil test is shown in Table 5-6-2.

i) Specific gravity test

Specific gravity of the soil particles is 2.59 to 2.66 and mean value is 2.62. The mean value of specific gravity of alluvial sand is approximately 2.70, so it is judged to be the average alluvial sand.

ii) The mean values of water content(W) and wet density(ρ_t) are shown in Table 5-6-3.

$\rho_d = 1.61$ is obtained by the calculation with the values shown above. ρ_d of alluvial sandy soil is generally 1.6 to 1.8, and the natural water content is 10 to 30. The data by actual test shows the comparatively high dry density and compact in comparison with above values. It is almost consistent with the result of penetration test.

iii) Grain size analysis

The grain size accumulation curve is shown in Fig.5-6-2. The grain size distribution is in the range of 0.005 mm to 10.0 mm. It shows mixed soil of silt to medium gravel. The grain size of 50% passing is almost fine sand to coarse sand.

About the grading, judging from the relationship between uniform coefficient(U_c) and coefficient of curvature(U_c'), grading is within the range shown below;

$$U_c = 32 > 10$$

$$U_c' = 0.5 < 1$$

It means that grading is not so good.

iv) Liquid limit and plastic limit test

5 samples were tested, but 2 samples could not be performed in plasticity test and they were N.P. Judging from the Fig.5-6-2, the samples include less silt

component. The mean values of the tests are shown below;

Liquid limit (L.L)	33.3 %
Plastic limit (P.L)	19.2 %
Natural water content (W)	20.4 %
Plastisity index (Ip)	14.1 %
Consistency index (Ic)	0.91

Compared with empirical data, plasticity index of alluvial silt is 10 to 30 % and consistency index is 1 ~ 2. Therefore, the nature of soil is less stable than that of ordinary alluvial silt.

v) Permeability test

The average of permeability coefficients is 3.93×10^{-3} cm/sec.

(3) Summary of the survey of foundation ground

The foundation ground in this site is evaluated by the data described above as the foundation of the tailing dam. There are several conditions met as the foundation of tailing dam. The conditions are shown below.

- ① To have necessary bearing capacity.
- ② Safe against sliding failure
- ③ No emanation of water

No emanation of water shown above in ③ was recognized by the field survey. As regard to ② safe against sliding failure is described in chapter "Stability Analysis", later. Here, the simple examination about ① is performed.

The maximum overloading of the dam is about 18 t/m^2 . The estimated subgrade reaction from N value of the foundation ground is 30 t/m^2 . The value of the bearing capacity of the ground in this site is enough.

5-6-2 Model of new tailing dam

A model of new tailing dam was already proposed in the previous report. In this report, examination was made again with consideration of stability of the slope. Based on the re-examination, the section shown in Fig. 5-6-3 was obtained. The outline of design of new tailing dam is described below.

(1) Inclination of slope

starting dam	upstream side	i=50 %
	downstream side	i=43.5 %
slope with spreaded soil		i=40.0 %

(2) Spreading soil on the slope(for prevention of dust scattering and scouring of surface)

covering by soil and vegetation

(3) Drainage

drainage for outside the dam ; channel along mountain slope
drainage for inside the dam ; inclined pipe
drainage for penetrated ground water ; collecting channel

(4) Dam height

the mean height	H=25 m
the height of initial embankment	H=11 m

(5) Dam volume approximately 300,000 m³

5-7 Summary of the Survey Results

This area is formed on Metasediments of Pre-tertiary Systems. The Magistral River passes through the area zigzagging from north to south. As a result of geological survey, it is likely that ground water also runs underground along this river. Thus, one observation hole, B-2, reached the high pressured water layer at a depth of around 105 m. This water can be supplied satisfactorily to a new mineral processing plant to be built in this area.

Since there exists no mining activity at present in and around this area, concentration levels of heavy metals in surface and ground water or soil samples are not as high as those of other survey areas, El Bote and Parral. Cyanide has never been detected in this El Coco area.

In the samples of surface water, Cd, Hg and Cr⁶⁺ are not detected. Among the other metals, Pb and As exceed the criterion limit of water supply standard by EPA in the samples of C-R6 and C-R5 respectively. These are regarded as natural

mineralization in this area.

In the samples of ground water heavy metal ions, except Cr^{6+} , were detected at higher levels than surface water. Among them Pb exceeds the criterion limit in almost all samples, especially high in C-B3. Arsenic exceeds the limit in the two samples, C-B1 and C-B7 situated near the faults found by the geological survey. It is possible that As is concentrated along the geological faults. More studies are yet to be done.

Arsenic is also concentrated at considerably high level in the soil samples taken in this area. This suggests the land is unlikely to fit for agricultural use.

These high levels of metal concentration are derived from natural mineralization in and around the survey area. Thus, it may be impossible to take some counterplans at present against the contamination. When a tailing dam is constructed inside the area, it is essential to prevent further contamination, which might be caused by effluent from the dam. To know the change in the environmental situation, another investigations shall be performed after mining activity starts.

As the results of soil property tests, the ground foundation of the proposed dam site was found suitable for construction. Based on these results a model tailing dam, which causes no pollution problems, was designed technically and economically for final recommendation.

5-8 Measures against Mine Pollution

As the result of the survey both in dry season and rainy season, attention must be paid to the following points in El Bote and Parral to make measures against mine pollution.

- (1) measures against collapse(upgrading of stability of slope)
- (2) measures against water pollution(installation of drainage)
- (3) measures against dust(eliminate the sources of dust)

New El Coco tailing dam is designed to realize these measures.

The detailed examination about the model section of new El Coco tailing dam (Fig.5-6-3) is described below.

5-8-1 Stability test of new tailing dam

Stability of the section shown in Fig.5-6-3 is described in this chapter.

The design aims to achieve safety factor over 1.2. The same standard and equation are used in the examination of stability test of the other tailing dams.

(1) Section of stability analysis

Model section for this stability test is shown in Fig.5-8-1. Boundary line of the basement layer was estimated with drilling data of B-11 and B-12.

Phreatic surface is estimated referring to the survey result of Parral and El Bote tailing dam.

(2) Soil constants

Soil constants for stability analysis were decided as follows;

① The same data used in the study of Parral were adopted here ,because no data about deposit-1 and deposit-2 are available in this site.

② surface soil (Zone- ②)

The soil excavated from the foundation of the dam is used as surface soil.

Soil constants by laboratory soil test are as follows;

$$G_s = 2.62 \quad w = 16.8 \% \quad \rho_t = 1.443 \text{ g/cm}^3$$

$$\rho_d = \rho_t / \left(1 + \frac{w}{100} \right) = 1.443 / \left(1 + \frac{16.8}{100} \right) = 1.235 \text{ g/cm}^3$$

$$e = (G_s / \rho_d) - 1 = (2.62 / 1.235) - 1 = 1.121$$

$$\begin{aligned} \rho_{sat} &= \rho_d + (1 - \rho_d / G_s) \\ &= 1.235 + (1 - 1.235 / 2.62) \\ &= 1.801 \text{ g/cm}^3 \end{aligned}$$

Shear strength is as follows;

$$\text{angle of shear resistance } \rho = 33.0^\circ$$

$$\text{cohesion } C = 5.0 \text{ tf/m}^2$$

③ gravelly soil (Zone- ④)

The same data used in the study of Parral and El Bote tailing dam were adopted as soil constants in this site, because of no testing data.

④ foundation ground (Zone- ⑤)

The same soil constants was adopted as those of surface soil.

(3) Other conditions

The horizontal seismic intensity during earthquake and the increment of circular arc(ΔR) were chosen as $K_h=0.15$ and $\Delta R=1.0$ m, respectively, as same as the other tailing dams.

(4) Calculation results

Calculation results of the model shown in Fig.5-8-1 is reviewed in Table 5-8-1.

The detailed result of stability analysis in ordinary condition is shown in Fig.5-8-2, and the arcs(or the arcs of which sliding plane locates at the deepest) which give minimum safety factor in each distance at that time is shown in Fig.5-8-3. The detailed results of stability analysis during earthquake($K_h=0.15$) and their arcs are shown in Fig.5-8-4 and Fig.5-8-5, respectively.

As the result, the minimum safety factor of this tailing dam satisfies the target value of over 1.2. Therefore, the stability of the model section shown in Fig.5-8-1 is stable against collapse.

5-8-2 Measure against Drainage Tailing Dam

To prevent the water through the tailing dam from flowing into the river or groundwater to pollute them, it is primarily necessary that the surface water due to rain must be avoided to directly contact the water in the dam which includes pollutants, and next to recover the polluted water. Or, if the dam surface is covered by soil which is not polluted, the surface water such as rain and the water outside of the dam is not polluted. In case of that, the surface water of the dam can be discharged into the river or be used as recycled water after the treatment. The flow chart of drainage of polluted water and not polluted water is shown in Fig.5-8-6.

The plan of drainage is shown in Fig.5-8-7.

(1) The capacity of drainage

The capacity of drainage is decided by the probable precipitation amount

for 100 years.

① The probable precipitation amount in a day

The orderly arranged data of precipitation in Concordia near El Coco by the daily amount of precipitation are shown in Table 5-8-2. The probable precipitation for 100 years is decided by plotting the probability in logarithm graph shown in Fig.5-8-8. The probable precipitation amount for 100 years is obtained as follows;

$$R_{24}=115 \text{ mm}$$

② Water collecting area

The water collecting area of each drainage in order to decide the capacity is as follows;

$$A_1=0.129 \text{ km}^2 \quad (\text{the southern slope of the dam})$$

$$A_2=0.018 \text{ km}^2 \quad (\text{stagnant water surface of the dam})$$

③ Run-off time

$$T_1=1.67 \times 10^{-3} (350 / \sqrt{0.25})^{0.7} = 0.16 \text{ h}$$

$$T_2=1.67 \times 10^{-3} (70 / \sqrt{0.02})^{0.7} = 0.13 \text{ h}$$

④ Average maximum intensity of precipitation

$$R_1 = \frac{115}{24} \left(\frac{24}{0.16} \right)^{2/3}$$
$$= 135 \text{ mm/h}$$

$$R_2 = \frac{115}{24} \left(\frac{24}{0.13} \right)^{2/3}$$
$$= 155 \text{ mm/h}$$

⑤ Calculation of design amount of floodwater

$$Q_{p1} = 1/3.6 \times 0.8 \times 135 \times 0.129 = 1.15 \text{ m}^3/\text{Sec}$$

$$Q_{p2} = 1/3.6 \times 1.0 \times 155 \times 0.018 \times 0.2 = 0.045 \text{ m}^3/\text{Sec}$$

The amount of overflow water

$$Q_{p4} = 5,200 \text{ m}^3/\text{month} = 0.002 \text{ m}^3/\text{Sec}$$

$$Q_{p2} = Q_{p3} + Q_{p4} = 0.155 + 0.002 = 0.157 \text{ m}^3/\text{Sec}$$

(2) Section of drainage

Each section of drainage calculated by design flood amount is as follows;

① Drainage of water outside of the dam (drainage along the mountain slope)

The section of drainage of water outside of the dam is assumed as in Fig.5-8-9(A);

$$Q = \frac{1}{0.015} \times 1.17 \times 0.38^{2/3} \times 0.02^{1/2}$$
$$= 5.79 \text{ m}^3/\text{sec} > Q_{P1} = 3.87 \text{ m}^3/\text{sec} \dots\dots\dots 0. K$$

According to the estimation, the section of the drainage is decided as in Fig.5-8-9(A).

② Drainage inside of the dam (slope gutter)

The section of drainage inside the dam is assumed as Fig.5-8-9(B);

$$Q = \frac{1}{0.015} \times 0.225 \times 0.160^{2/3} \times 0.05^{1/2}$$
$$= 0.99 \text{ m}^3/\text{sec} > 0.157 \text{ m}^3/\text{sec}$$

According to the estimation, the section of the drainage is decided as in Fig.5-8-9(B).

5-8-3 Measure against Powder Dust Scattering

The origin of dust is particles of sand and silt which were dried up in the dry season in El Bote and Parral tailing dam. The covering with soil on the slope and making vegetation on it prevents dust scattering. The measure is also effective to prevent surface from scouring due to rainfall in the rainy season.

5-8-4 Measures against Groundwater Pollution

According to hydraulic observation, groundwater is abundantly stored along fault zones and in permeable terrace deposits. The fault zones and the terrace deposits are well developed along the Magistral river and ex-river of planned tailing dam area.

The tailing dam construction guide line of Japan is referred to design this

new El Coco tailing dam in article 5-8-1 and 5-8-2, in which an engineering method for drainage system is described to prevent tailing-rainwater contamination and waste water infiltration. On the other hand, a hydraulic method, described in article 5-4-3 in which groundwater flow systems are simulated, is recommended as a counterplan to reduce construction cost. The hydraulic method is the second countermeasure to prevent groundwater pollution. This method utilizes flow system between waste water and groundwater, in which system waste water infiltrates underground and mixed with groundwater. The groundwater is pumped up from the bore hole near the new tailing dam to use for slime transport. This waste water recycle system is adequate to prevent groundwater pollution and to use groundwater efficiently below the planned new tailing dam.

The water for living supply is should be used from boring well B-2, from which groundwater discharged at the rate of $120\text{m}^3/\text{day}$.

It is not necessary for the hydraulic counterplan to set up the drainage system described in article 5-8-2, but to set up water recycle system economically. This system is composed of two bore holes for pumping, trench around the tailing dam and a deposition pond to collect surface runoff water as Fig.5-4-9 shows. The groundwater for drink is used from bore hole B-2 of the Magistral river side.

We suggest that to take much volume of groundwater which is not polluted by waste water of tailings by making pumping up well along the Magistral river in the future, that will be constructed by the same manner of construction and best-site finding survey of our project team done.

5-8-5 Work Program and Construction Cost of the Model Tailing Dam

The model tailing dam is based on upstream depositing system, which has traditionally been adopted in Mexico. Consequently, routine costs for slime depositing is excluded from the following estimation.

(1) Work Program

Work program is illustrated in the figure shown below.

Type of Work	Amount	5month	10month	15month	20month
Basic Groundwork	20,000 m ³	2month			
Starting Dam Piling Work	65,000 m ³	4 month			
Rubble Filter Work	3,000 m ³			0.6 month	
Drainage Inside The Dam	900 m	5 month			
Drainage Outside The Dam	510 m	3 month			
Underdrainage Work	730 m	0.6 month			

(2) Construction Cost

According to the construction basis in Japan, total costs are estimated as follows.

Type of Work	Amount	Unit Cost (US\$)	Total Cost (US\$)
Countermeasures against Dam Collapse and Dust Problem			
Basic Groundwork	20,000 m ³	2.6	52,000
Starting Dam Piling Work	65,000 m ³	5.6	364,000
(Sub Total)			(416,000)
Drainage			
Inside the Dam	900 m	140.0	126,000
Outside the Dam	510 m	186.7	95,000
Underdrainage	730 m	100.0	73,000
(Sub Total)			(294,000)
TOTAL			710,000

(3) Specification of Work

Specification of the works and necessary equipment are listed in the following Table.

Type of Work	Equipment	Unit Capacity	Unit
Basic Groundwork			
Excavation and loading	Backhoe (1.0m ³ class)	68 m ³ /h	1
Transportation	Dumptruck (11t class)	33 m ³ /h	2
Spread and Roll	Bulldozer (21t class)	68 m ³ /h	1
Starting Dam Piling Work			
Rock excavation at borrow pit	Bulldozer with Ripper (32t class)	53 m ³ /h	1
Loading of crushed rock	Backhoe (1.0m ³ class)	51 m ³ /h	1
Transportation	Dumptruck (11t class)	17 m ³ /h	2
Spread and Roll	Bulldozer (21t class)	64 m ³ /h	1

Remarks

1. Transportation during the Basic Groundwork is estimated as 500m.
2. Transportation during the Starting Dam Piling Work is estimated as 300m.
3. Working hours are 7 hours a day and working days are 25 days per month.



Fig. 5-1-1 Hydrologic and Meteorologic Map

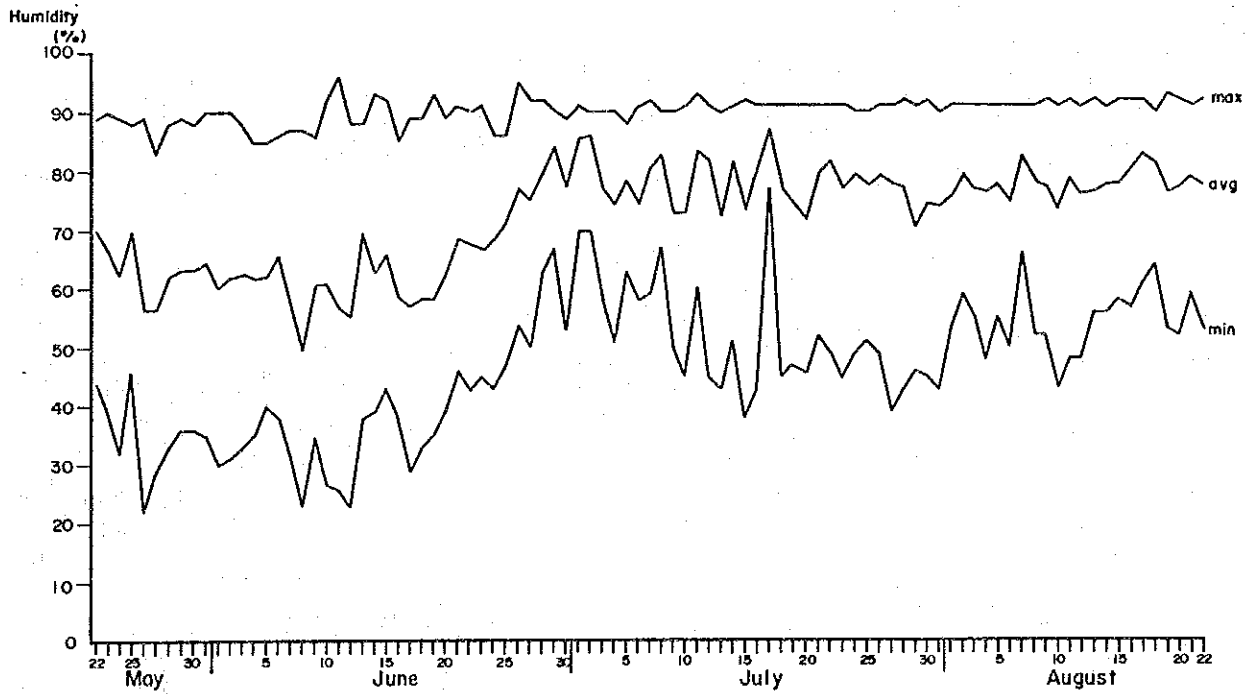
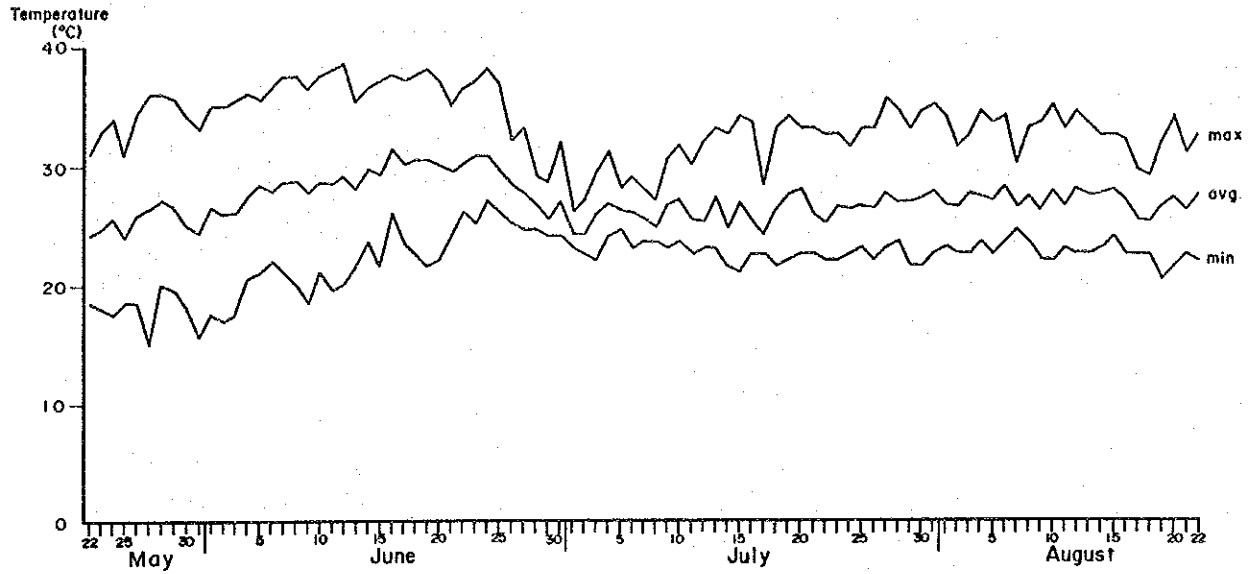


Fig. 5-1-2. Temperature-Humidity Variation Diagram

Geological Age	Symbol	Explanation	
Quaternary	Recent	Q1	Talus deposits
		Qr1	River deposits
		Qr2	Recent terrace deposits
	Pleistocene	Pt1	Pleistocene lower terrace deposits
		Pt2	Pleistocene middle terrace deposits
Pt3		Pleistocene upper terrace deposits	
Tertiary	Ta	Altered acidic rocks	
	Tp	Toba pyroclastic rocks	
	Te	Extrusive rocks : andesite	
	Ti	Intrusive rocks : porphyrite	
	Td	Intrusive rocks : dacite	
Pre-Tertiary		Slate partly intercalated with sandstone	
		Fault	



Fig. 5-2-1 Geological Plane Map (New El Coco)

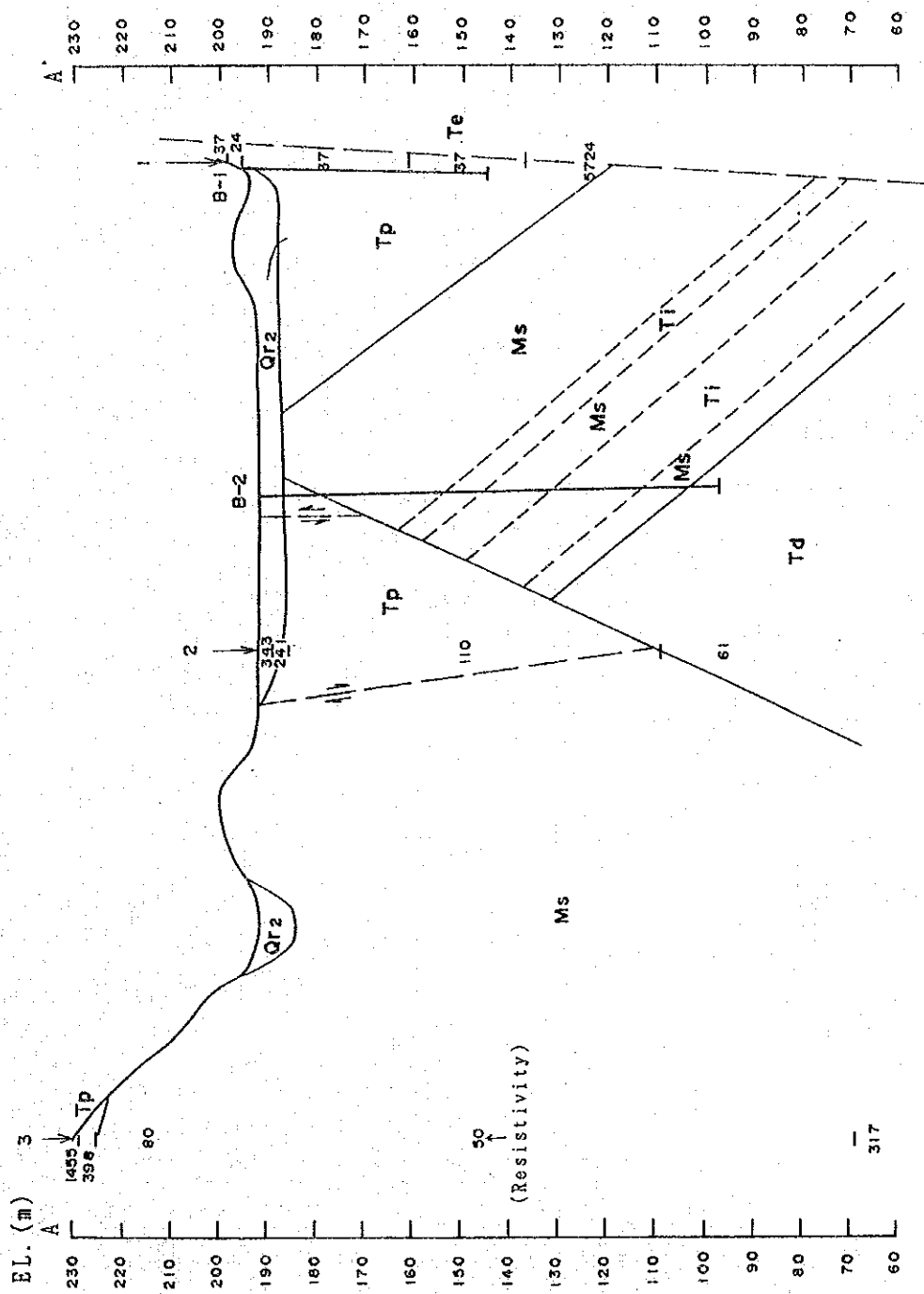


Fig. 5-2-2 Geological Cross Section (New El Coco) (1)

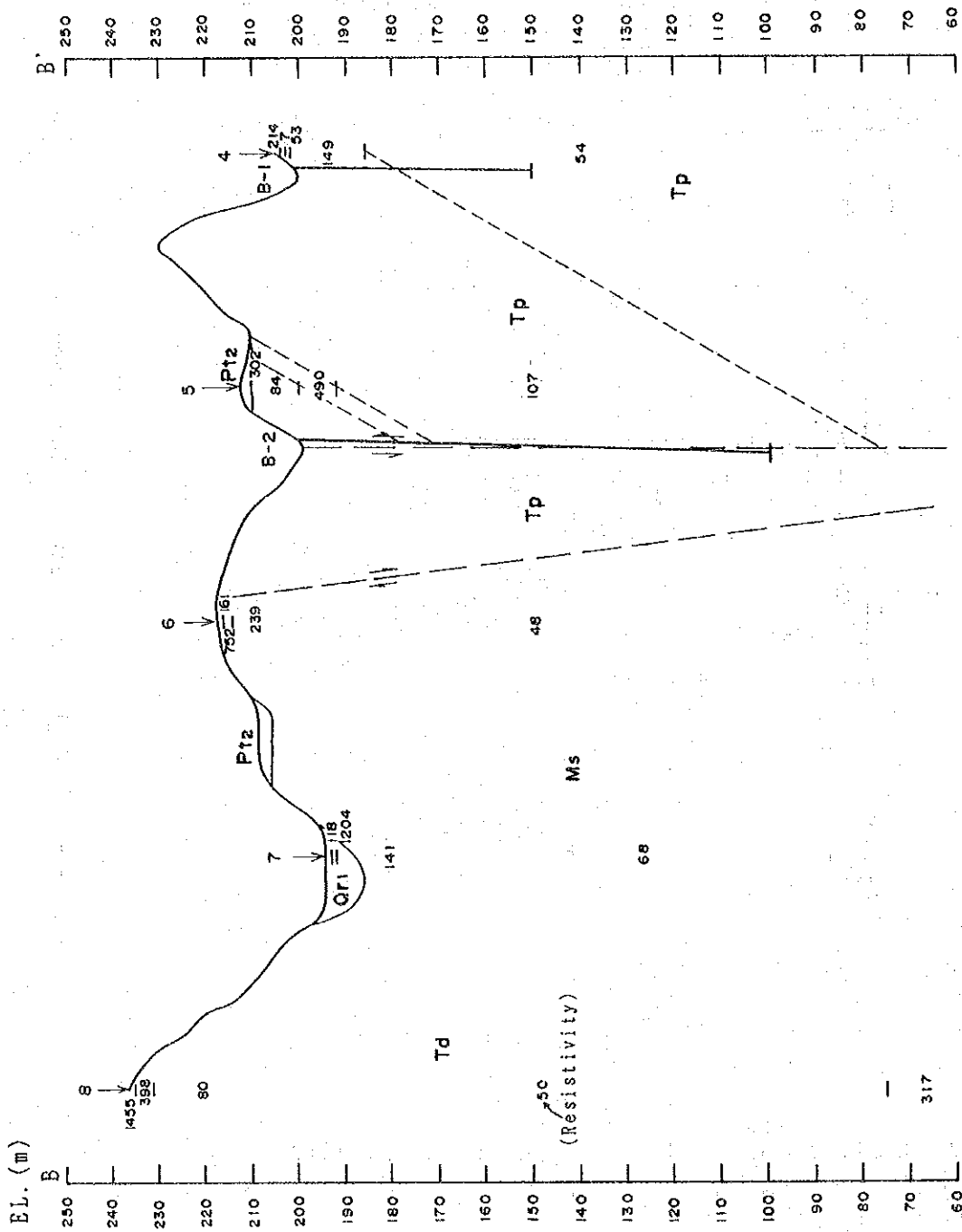


Fig. 5-2-2 Geological Cross Section (New El Coco) (2)

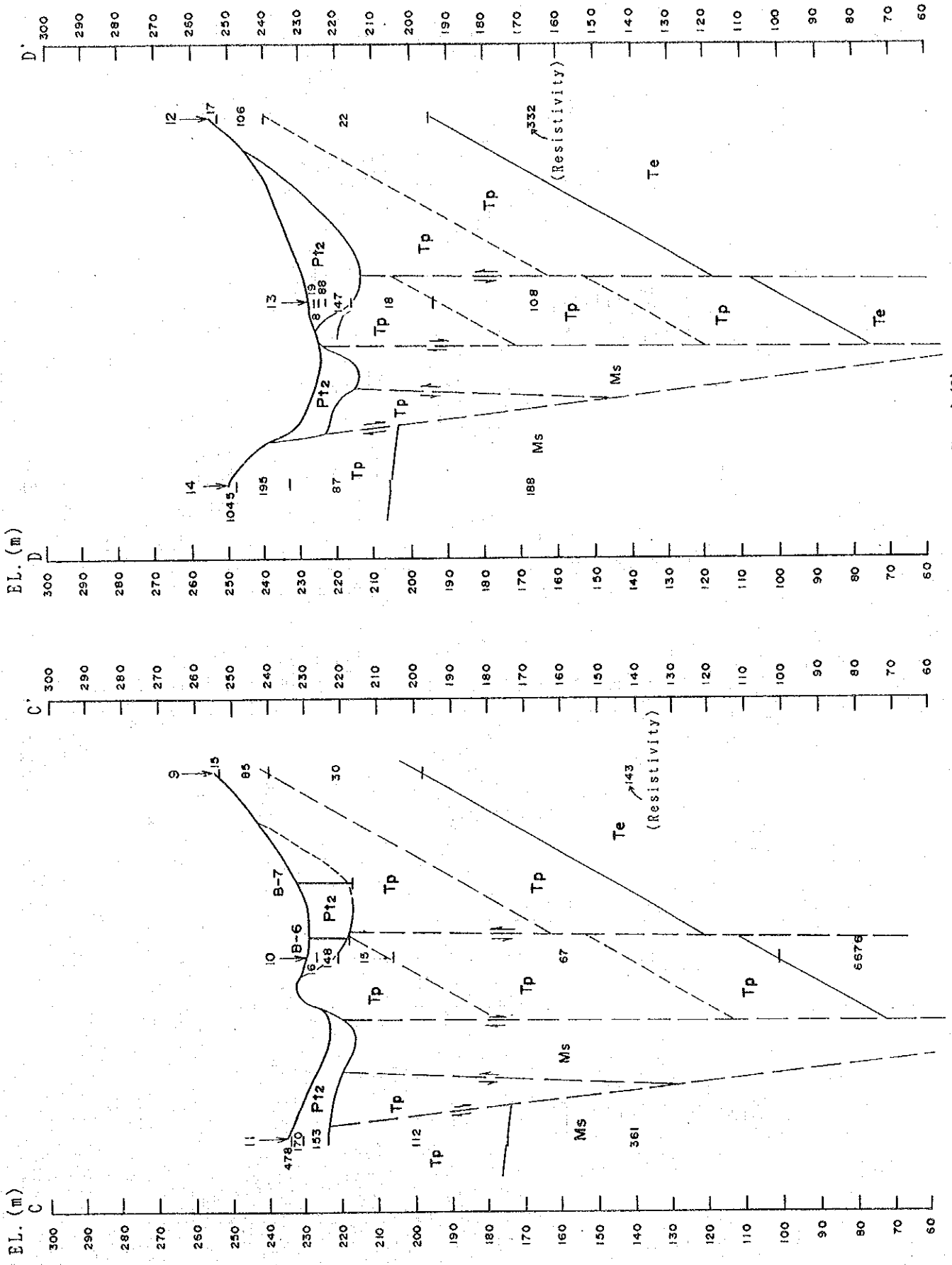


Fig. 5-2-2 Geological Cross Section (New El Coco) (3)

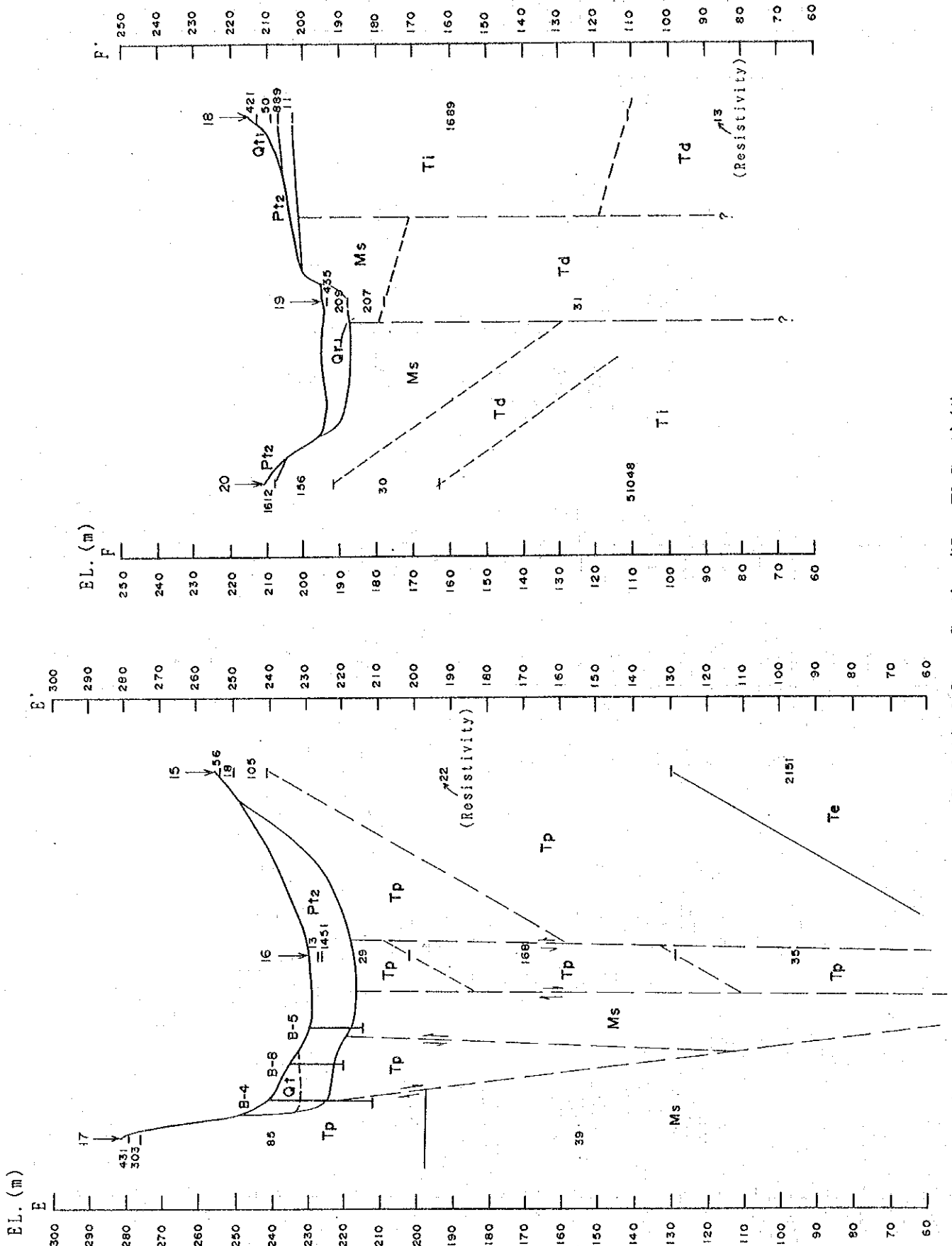


Fig. 5-2-2 Geological Cross Section (New El Coco) (4)

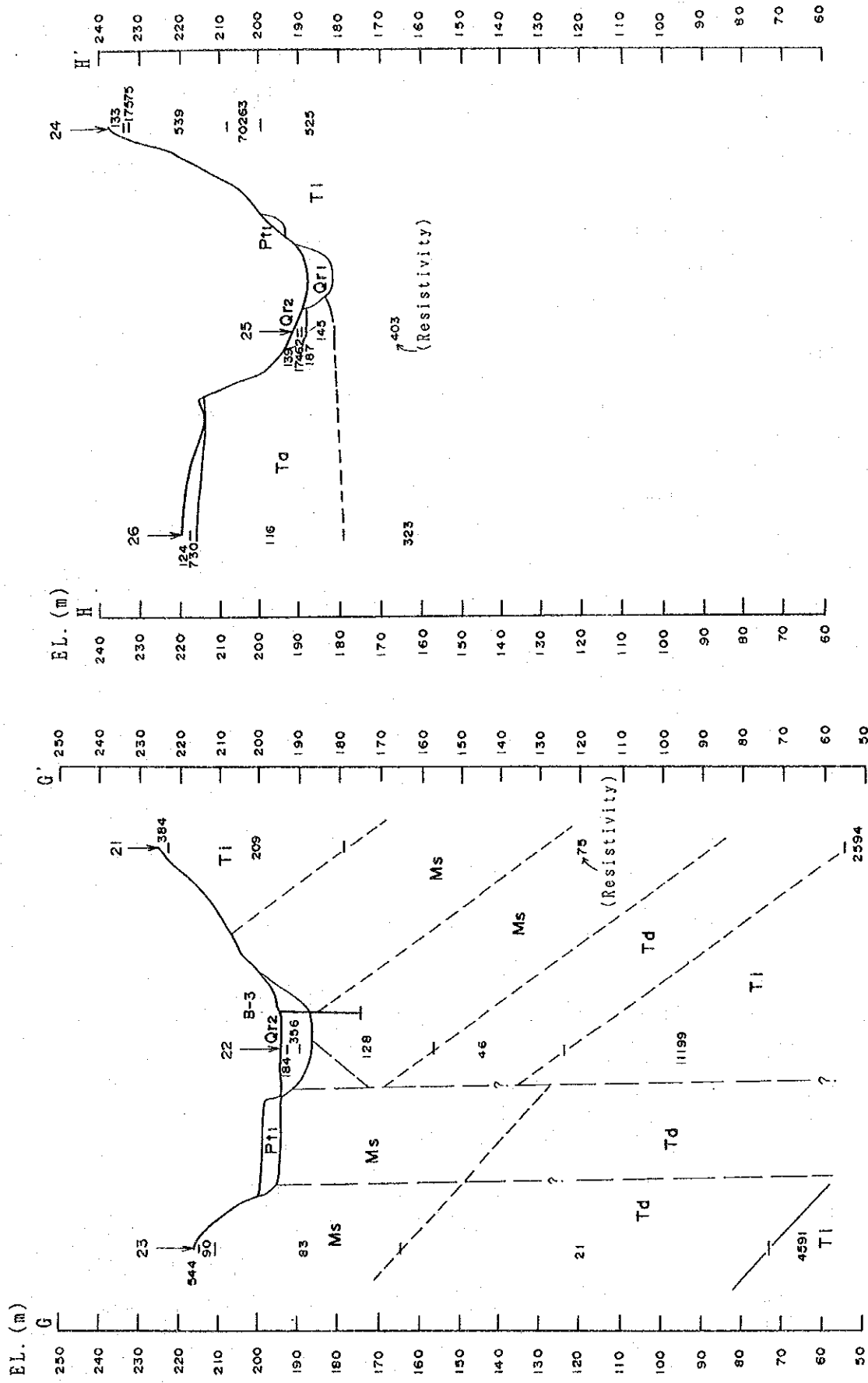


Fig. 5-2-2 Geological Cross Section (New El Coco) (5)

(3) New El Coco

Geological Age		Symbol	Explanation
Quaternary	Recent	Qt	Talus deposits
		Qr1	River deposits
		Qr2	Recent terrace deposits
	Pleistocene	Pt1	Pleistocene lower terrace deposits
		Pt2	Pleistocene middle terrace deposits
		Pt3	Pleistocene upper terrace deposits
Tertiary	Ta	Altered acidic rocks	
	Tp	Toba pyroclastic rocks	
	Te	Extrusive rocks ; andesite	
	Ti	Intrusive rocks ; porphyrite	
	Td	Intrusive rocks ; dacite	
Pre-Tertiary		Slate(partly intercalated with sandstone)	
		—	Fault

Fig. 5-2-3 Geologic Column (New El Coco)

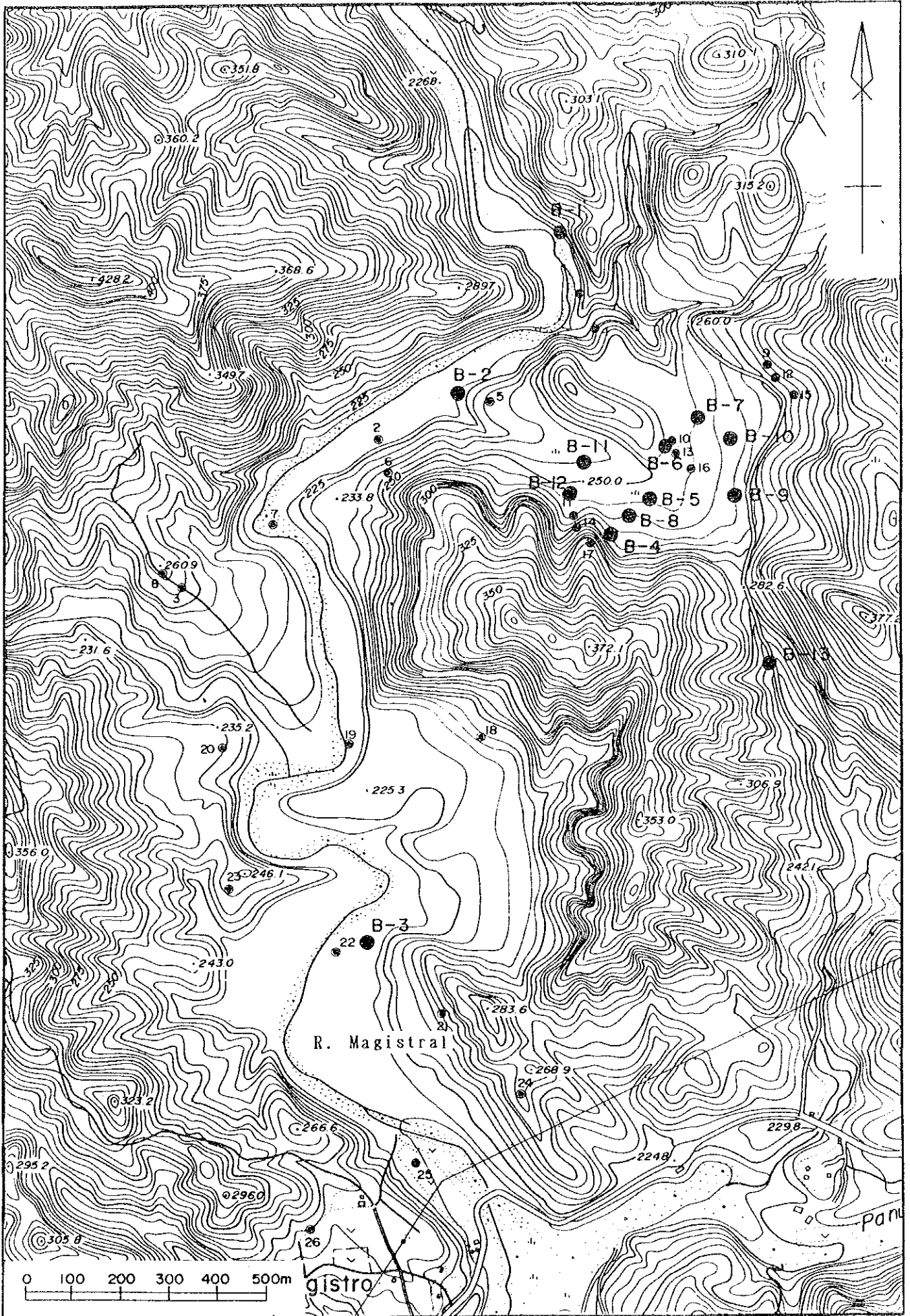


Fig. 5-2-4 Location Map of Boring Site

Depth (m)	Drilling Log	Formation	Lithology	Description	Core Shape					Water Flow (cm/sec)		Water Level Lost Circulation	
					<20 cm	10-20cm	5-10cm	2mm - 5cm	> 2 mm	Dry Season	Rainy Season		
0.00		Surface soil	silty sand	This layer consists of dark reddish brown, unconsolidated, poorly sorted and silty sand with gravel. The gravel is composed of subangular dacite and andesite, which is less than 3cms in size.									
2.40		Recent terrace deposits	gravel	The gravel consists of rounded or subrounded fragments of dacite, pumice, andesite and granodiolite, which is 5cms in the mean diameter and 32cms at the largest size. The matrix is composed of light yellowish gray, poorly sorted and medium to coarse-grained sand.									
8.25		Toba pyroclastic rocks	andesite	The andesite is purplish gray, porphyritic and altered. A numerous of irregular joints have occurred by tension, and calcite veins have developed along them. Partly, few shear joints are present. 8.55m: shear joint; dip angle 66°.									
10.65			tuff	This tuff is purplish gray and coarse-grained. Graded bedding has weakly developed. This layer contains angular gravels of andesite, ranging in size 1 to 2cms, and gravels has general tendency to become much more toward the bottom in this layer.									
12.00													

Fig. 5-2-5 Boring Log (1)

Depth (m)	Drilling Log	Formation	Lithology	Description	Core Shape					Water Flow (cm/sec)		Water Level Lost Circulation
					<20 cm	10-20cm	5-10cm	2mm - 5cm	> 2 mm	Dry Season	Rainy Season	
12.00	[Symbol]		tuff	This is the same rock above mentioned.					0.51			
13.60									0.99	0.40 (8/20) 0.51 (8/6) 0.40 (8/26)		
14.40	[Symbol]	Toba pyroclastic rocks	tuff breccia	The tuff breccia is purplish gray and andesitic.					0.69	0.40 2.05 0.40		
14.80									0.57	0.40 2.76 1.22		
18.00~19.90	[Symbol]		tuff breccia	Calcite veins have developed like as reticulation.					0.40	0.40 2.88 0.87		
21.00~22.00									0.69	0.40 3.00 1.11		
22.25~22.30	[Symbol]		tuff breccia	Calcite veins has developed densely.					0.51	0.40 2.05 0.75		
23.00									0.51	0.40 1.58 0.40		
24.00	[Symbol]			Shear joints; dip angle 65° and 85°. Striation & slickenside have occurred on joint surface, and calcite veins have developed along joint.					0.40	0.40 0.40 0.40		

Fig. 5-2-5 Boring Log (2)

Depth (m)	Drilling Log	Formation	Lithology	Description	Core Shape					Water Flow (cm/sec)		Water Level Lost Circulation	
					<20 cm	10-20cm	5-10cm	2mm-5cm	>2 mm	Dry Season	Rainy Season		
24.00	△ △ △ △ △ △ △ △ △ △ △ △		tuff breccia	This is the same rock above mentioned.						0.45			
											0.40 1.82 1.58	{8/20} {8/8} {7/26}	
										0.69			
											0.40 0.98		
										1.52			
											0.40 0.63		
										0.40			
27.50	△ △	Toba pyroclastic rocks	lapilli tuff	The lapilli tuff is pale purplish gray and mainly includes of reddish brown, angular or subangular gravels of andesite, ranging in size 0.2 to 1.5cms. 29.40~31.00m Shear joints; dip angle 50° and 80°. Striation and slickenside have developed on joint surface. 31.20~32.70m Vertical joint has developed.							0.81	0.40 1.11 0.51	
											0.40 0.87 0.40		
										1.11			
											0.40 0.63 0.51		
										0.40			
											0.40 0.63 0.40		
										0.45			
											0.40 0.40 0.40		
										0.40			
											0.40 0.40 0.40		
										0.45			
											0.40 0.40 0.40		
33.20	△ △ △ △ △ △ △ △ △ △ △ △		tuff breccia	The tuff breccia is purplish gray and andesitic. The texture is not clear by alteration. Calcite veins have developed as a whole in the bed.							0.45	0.40 0.40 0.40	
											0.40 0.40 0.40		
										0.45			
											0.40 0.40 0.40		
										0.40			
											0.40 0.40 0.40		
36.00	△ △ △										0.40 0.40 0.40		

Fig. 5-2-5 Boring Log (3)

Depth (m)	Drilling Log	Formation	Lithology	Description	Core Shape					Water Flow (cm/sec)		Water Level Lost Circulation
					<20 cm	10-20cm	5-10cm	2mm-5cm	> 2 mm	Dry Season	Rainy Season	
36.00	△ △			This is the same rock above mentioned.						0.40		
	△										0.40	
	△ △									0.40	0.40	(8/20)
	△									0.40	0.40	(8/8)
	△ △									0.40	0.40	(7/26)
	△											
	△ △									0.40	0.40	
	△									0.40	0.40	
	△ △									0.40	0.40	
	△											
39.00	△ △									0.40	0.40	
	△											
	△ △									0.40	0.40	
40.00	△									0.40	0.40	
	△ △											
	△											
	△ △									0.51	0.40	
	△											
	△ △									0.99	0.40	
	△											
	△ △									0.51	0.51	
	△											
	△ △									0.87	0.99	
	△									0.40	0.40	
	△ △											
	△											
	△ △									0.40	0.40	
	△											
	△ △									0.40	0.40	
	△											
45.00	△ △									0.40	0.40	
	△											
	△ △									0.40	0.40	
	△											
	△ △									0.40	0.40	
	△											
	△ △									0.40	0.40	
	△											
	△ △									0.45	0.40	
	△											
48.00	△ △									0.40	0.40	
										0.40	0.40	
										0.40	0.40	

Fig. 5-2-5 Boring Log (4)

Depth (m)	Drilling Log	Formation	Lithology	Description	Core Shape					Water Flow (cm/sec)		Water Level Lost Circulation
					<20 cm	10-20cm	5-10cm	2cm ~ 5cm	>2 mm	Dry Season	Rainy Season	
48.00	△ △ △ △ △ △ △ △	Toba pyroclastic rocks	tuff breccia	This is the same rock above mentioned. 48.50m Shear joint; dip angle 30° and 80°.						0.40		
49.85~50.00m	△			This part is dark purplish gray and andesitic.						0.40	0.40	(8/6)
50.00	△											

Fig. 5-2-5 Boring Log (5)

Depth (m)	Drilling Log	Formation	Lithology	Description	Core Shape					Water Flow (cm/sec)		Water Level Lost Circulation
					<20 cm	10-20cm	5-10cm	2mm - 5cm	> 2 mm	Dry Season	Rainy Season	
0.00		Surface soil	silty sand	This layer consists of light grayish brown, unconsolidated, poorly sorted and silty sand with gravel. The gravel is composed mainly of rounded andesite which is 1 to 3cms in diameter.							0.75 0.40 0.40 0.40	(3/15) pH 8.87
1.40		Recent terrace deposits	gravel	The gravel chiefly consists of rounded, subrounded or subangular fragments of andesite and tuff breccia which is 2 to 3cms in the mean diameter and 80cms at the largest size. The matrix is the same of upper layer.						0.40	0.40 0.40 0.40	(7/25) (8/5) (8/7) (8/20)
3.20			gravelly sand	The gravel consists of rounded fragments of andesite and granodiorite, ranging in size 3 to 5cms. The matrix is well sorted and very coarse-grained sand.								
3.80			sand	The sand is moderately well sorted and medium to coarse-grained, as a whole. 5.00~5.10 m: The lowest part is accompanied with many gravels of andesite and tuff which is 2 to 5cms in diameter.						0.51	0.40 0.40 0.40	
5.10			Toba pyroclastic rocks	tuff	The tuff is pale greenish gray and altered. This layer has undergone chloritization, silicification and mineralization, so that chlorite, quartz and pyrite have occurred along the joint. 5.40m Shear joint; dip angle 60°. Striation has developed. 5.70~7.70m This part is light gray. 7.20m Shear joint; dip angle 45°. Striation has developed. 7.30m Shear joint; dip angle 60°. Striation has developed.						0.75	0.40 0.40 0.51
7.70		Filling sediments	sand	The sand is light gray, unconsolidated, well sorted and medium-grained, and it derived from recent fluvial deposits.						0.63	0.40 0.40 0.40	
8.20		Toba pyroclastics	tuff	This is the same rock above mentioned.								
8.40		Fault	fault breccia	The breccia is black and fragile. The fragment has formed like a blade. Striation and slickenside have occurred on the surface of fragments. (shear joint; dip angle 30°)								
8.70		Filling sediments	sand	The sand is light gray, unconsolidated, well sorted and fine-grained, and it derived from recent fluvial deposits.						0.40	0.40 0.40 0.40	
10.00		Fault	fault breccia	This is the same fault breccia above mentioned. (shear joint; dip angle 60°)								
10.30		Toba pyroclastic rocks	tuff	The tuff is white and coarse-grained, and characteristically includes quartz grains. This layer has undergone silicification and mineralization, so that the texture is not clear and pyrite occurs as small cubes in tuff. 11.00m Shear joint; dip angle 35°.						0.40	0.40 0.40 0.40	
12.00												

Fig. 5-2-5 Boring Log (6)

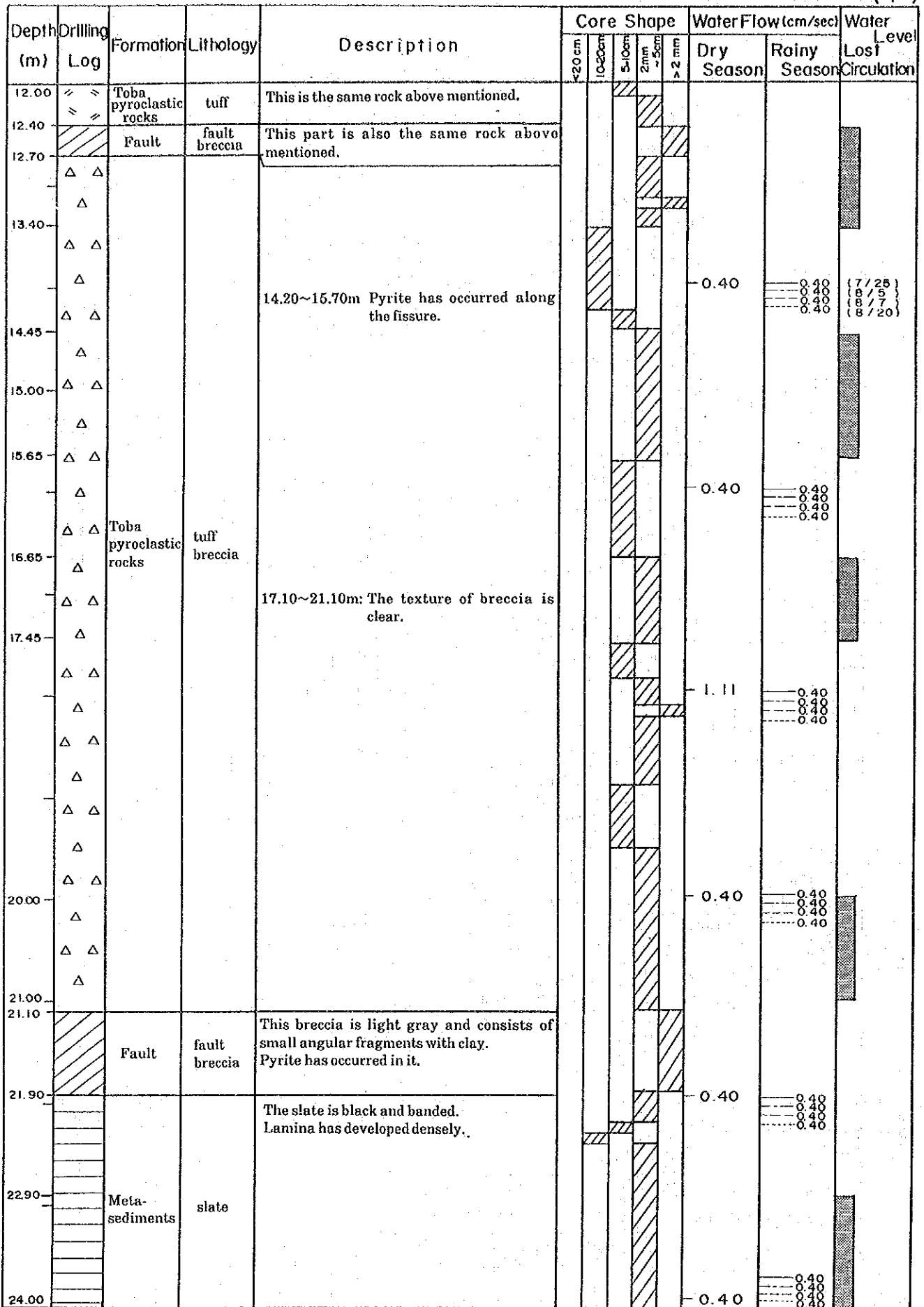


Fig. 5-2-5 Boring Log (7)

Depth (m)	Drilling Log	Formation	Lithology	Description	Core Shape					Water Flow (cm/sec)		Water Level Lost Circulation
					<20 cm	10-20cm	5-10cm	2mm	3cm	2 REE A	Dry Season	
24.00			slate	This is the same rock above mentioned.								
25.30			sandstone	This is composed of light gray and medium-grained sandstone. This layer is loose.								
25.60			slate	The slate is grayish white and altered. This layer has undergone chloritization and mineralization, so that chlorite and pyrite have occurred in it. And also, a numerous of shear joints developed in this layer.					0.40	0.40 0.40 0.40 0.40	(7/25) (8/5) (8/7) (8/20)	
25.70				25.90m Lamina; dip angle 25°. 26.70m Shear joint; dip angle 65°. Slickenside developed on the joint surface.					0.40	0.40 0.40 0.40 0.40		
28.80			sandstone	28.80~29.00m Shear joints; dip angle 40° and 50°.					0.40	0.40 0.40 0.40 0.40		
29.80		Meta-sediments		The sandstone is light gray, well sorted and fine-grained. This layer is loose, because of the matrix has been washed away by underground water flow.					0.40	0.40 0.51 0.40 0.40		
31.20			slate	This part is gray.					0.75	0.40 0.40 0.40 0.40		
				34.00~35.20m This part is intercalated with some thin beds of sandstone.					0.63	0.40 0.40 0.40		
36.00	L L	Intrusive rocks	porphyrite	The porphyrite is gray and white-spotted. This rock is characterized by abundant megaphenocrysts of feldspar ranging up to 1cm in diameter. Pyrite has occurred in it.					0.40	0.40 0.40 0.40		

Fig. 5-2-5 Boring Log (8)

Depth (m)	Drilling Log	Formation	Lithology	Description	Core Shape					Water Flow (cm/sec)		Water Level Lost Circulation				
					<20 cm	10-30 cm	5-10 cm	2mm - 5mm	2mm A	Dry Season	Rainy Season					
36.00	L L	Intrusive rocks	porphyrite	This is the same rock above mentioned.												
	L															
	L L															
	L															
	L L															
	L															
38.10	L L															
	L															
38.80	L L															
	L															
	L L															
	L															
40.10	L L															
	L															
	L L															
	L															
41.50	L L															
	L															
	L L															
	L															
42.35	L			42.20m joint; dip angle 55°.												
		Meta-sediments	slate	42.35~43.40m This part is gray and has undergone mineralization. Veins of calcite and pyrite have occurred like as reticulation, and partly, galena has accompanied pyrite.												
43.40																
						43.30m Shear joint; dip angle 35°. Joint surface is black.										
						44.30m Lamina; dip angle 40°.										
						44.35m Shear joint; dip angle 40°. Pyrite has occurred along the joint which has striation.										
44.55																
45.55																
48.00																

Fig. 5-2-5 Boring Log (9)

Depth (m)	Drilling Log	Formation	Lithology	Description	Core Shape					Water Flow (cm/sec)		Water Level Lost Circulation
					<20 cm	10-20cm	5-10cm	2mm ~ 5cm	> 2 mm	Dry Season	Rainy Season	
48.00				This is the same rock above mentioned.								
48.20m				Lamina; dip angle 30°. Shear joint; dip angle 25°. Striation has developed on this surface.						3.41	4.89 0.40 5.72 7.85	(7/25) (8/5) (8/7) (8/20)
49.75										5.01	4.00 0.40 5.01 5.37	
										5.07	4.54 4.89 4.54 7.14	
		Meta-sediments	slate							5.13	0.40 4.89 4.77 7.50	
52.55												
52.70m				Lamina; dip angle 50°. Shear joint; dip angle 60°. Striation has occurred on this surface with pyrite skin.						1.05	0.40 4.56 4.94 5.48	
										0.40	0.40 4.77 0.40 4.77	
										0.45	0.40 4.18 0.40 1.46	
										2.94	0.69 3.01 0.51 5.25	
56.30				This porphyrite is dark greenish gray and is characterized by megaphenocrysts of feldspar.								
56.30~61.40m				Megaphenocrysts of feldspar are only a few in this part.						0.99	0.45 4.30 0.40 1.22	
										4.95	0.51 4.42 0.40 6.37	
		Intrusive rocks	porphyrite									
											0.40 0.40 0.40 5.13	
59.60												
60.00												

Fig. 5-2-5 Boring Log (10)

Depth (m)	Drilling Log	Formation	Lithology	Description	Core Shape					Water Flow (cm/sec)		Water Level Lost Circulation
					<20 cm	10-20cm	5-10cm	2cm	1-5cm	2 m E A	Dry Season	
96.90			Intrusive acidic rocks dacite	This is the same rock above mentioned.								
105.00												

Fig. 5-2-5 Boring Log (11)

Depth (m)	Drilling Log	Formation	Lithology	Description	Core Shape					Water Flow (cm/sec)		Water Level Lost Circulation		
					<20 cm	10-20cm	5-10cm	2mm	< 5cm	> 2 mm	Dry Season		Rainy Season	
84.00	[Drilling Log Pattern]			This is the same rock above mentioned. 84.70m Foliation; dip angle 70°.										
87.50				86.40~105.00m Core shape is smaller than upper part.										
96.00				Intrusive acidic rocks dacite	95.00~105.00m Core shape looks like sand or clay.									

Fig. 5-2-5 Boring Log (12)

Depth (m)	Drilling Log	Formation	Lithology	Description	Core Shape					Water Flow (cm/sec)		Water Level Lost Circulation
					<20 cm	10-20cm	5-10cm	2mm ~ 5cm	2 mm A	Dry Season	Rainy Season	
60.00	L L			This is the same rock above mentioned.								
	L											
	L L											
	L											
	L L											
	L											
	L L											
	L			62.80m Joint; dip angle 55°.								
	L L			63.20m Shear joint; dip angle 55°. Striation has occurred on this surface.								
	L											
	L L			64.30m Foliation; dip angle 45°.								
	L											
65.00	L L											
	L	Intrusive rocks	porphyrite									
	L L											
	L											
	L L											
	L											
	L L											
	L											
	L L											
	L			68.40m Foliation; dip angle 55°.								
	L L			68.60m Joint; dip angle 60°.								
	L											
	L L											
	L											
	L L											
	L			70.90m Shear joint; dip angle 35°. Striation and calcite vein has occurred.								
	L L											
	L			72.00m Shear joint; dip angle 5°. Striation and calcite vein has occurred.								
72.00	L L											

Fig. 5-2-5 Boring Log (13)

Depth (m)	Drilling Log	Formation	Lithology	Description	Core Shape					Water Flow (cm/sec)		Water Level Lost Circulation
					<20 cm	10-20cm	5-10cm	2mm - 5cm	> 2 mm	Dry Season	Rainy Season	
72.00	L L	Intrusive rocks	porphyrite	This part is dark gray and hard, and also it's characterized by very few megaphenocrysts of feldspar, like as diabase.	[Core shape diagram]							
73.00	L L											
74.00	L L											
74.50	L L											
74.50	[Wavy pattern]	Meta-sediments	slate	The slate is gray and a numerous of joints has occurred along the lamina. 74.00~74.50m This part has undergone mineralization. Quartz veins have occurred with pyrite. 76.10m Shear joint; dip angle 45°. Striation has occurred on this surface. 76.80m Joint, dip angle 90°.	[Core shape diagram]							
78.10m	Lamina; dip angle 50°.											
79.70	[Wavy pattern]											
80.00	[Wavy pattern]											
82.90	[Wavy pattern]											
82.90	[Vertical dashes]	Intrusive acidic rocks	dacite	The dacite is grayish white to white and altered. And also it's characterized by abundant phenocrysts of quartz ranging in size 2 to 3mms.	[Core shape diagram]							
84.00	[Vertical dashes]											

3/16
120
t/day

Fig. 5-2-5 Boring Log (14)

Depth (m)	Drilling Log	Formation	Lithology	Description	Core Shape					Water Flow (cm/sec)		Water Level Lost Circulation			
					<20 cm	10-20 cm	5-10 cm	2mm - 50mm	2 mm A	Dry Season	Rainy Season				
0.00		Surface soil	gravelly silt	The gravel mainly consists of rounded andesite and tuff breccia fragments. The matrix is composed of light grayish brown sandy silt.											
1.10			sandy silt	This layer consists of dark brown sandy silt.											
2.35		Recent terrace deposits	gravelly silt	This layer is composed chiefly of light gray to light yellowish gray silt which contains gravels of slate ranging in size 0.2 to 1cm.								2.35 m ▽ (3/16) pH 8.71			
4.00			gravelly sand	The gravel mainly consists of rounded slate and andesite fragments ranging in size 0.3 to 5cms. The matrix is the same of upper layer.											
4.90			gravel	The gravel chiefly consists of rounded slate and sandstone fragments ranging 2 to 3cms in the mean diameter and 7cms at the largest size.											
8.40		Meta-sediments	slate	The slate is black, and it's accompanied with calcite veins and pyrite cubes.											
10.10			sandstone	This rock is gray, hard and medium-grained. there is lamina in it, and pyrite has occurred along the joint.											
		Fault	fault breccia	This is black and slaty, and contains pyrite as cubes. Striation and slickenside have developed on the surface of fragments.											
		Meta-sediments	sandstone	This rock is gray and fine-grained.											

Fig. 5-2-5 Boring Log (15)

Depth (m)	Drilling Log	Formation	Lithology	Description	Core Shape					Water Flow (cm/sec)		Water Level Lost Circulation		
					<20 cm	10-20cm	5-10cm	2mm - 5cm	> 2 mm	Dry Season	Rainy Season			
12.00	[Dotted pattern]	Meta-sediments	sandstone	This is the same rock above mentioned.							0.40	(7 / 25)		
13.00~20.00m				This part contains lots of pyrite cubes.						0.40	0.40	(8 / 6)	(8 / 20)	
14.50m				Joints; dip angle 85° and 90°. Pyrite skin has covered on the surface of joints.							0.40	0.40		
18.40~19.00m				This part contains abundant gravels of slate ranging 0.1 to 0.2cm in diameter.								0.40	0.40	
18.80m				Lamina; dip angle 10°.								0.40	0.40	
19.00~20.00m				This part has strongly undergone alteration								0.40	0.40	
												0.40	0.40	
												0.40	0.40	
												0.40	0.40	
												0.40	0.51	
20.00														

Fig. 5-2-5 Boring Log (16)

Depth (m)	Drilling Log	Formation	Lithology	Description	Core Shape					Water Flow (cm/sec)		Water Level Lost Circulation
					< 20 cm	10-20 cm	5-10 cm	2mm - 5cm	> 2 mm	Dry Season	Rainy Season	
0.00	o o	Surface soil	sand and gravel	<p>This gravel mainly consists of grayish white, angular or subangular acidic tuff which is 2 to 4cms in the mean diameter and strongly weathered.</p> <p>The matrix is composed of pale yellowish brown, unconsolidated and poorly sorted sand with silt.</p> <p>This layer is derived from talus deposits.</p>								
2.30	o o o o o o o o			gravelly sand	<p>The gravel chiefly consists of grayish white, angular or subangular, and weathered acidic tuff which is less than 2cms in diameter.</p> <p>The matrix is composed of brown, very poorly sorted and silt-rich sand, and weakly consolidated.</p>							
3.80	o o	Talus deposits	sandy silt	<p>The gravel mainly consists of grayish white, angular or subangular, and weathered acidic tuff which is less than 3cms in diameter.</p> <p>The matrix is made up of light gray and weakly consolidated silt which is contained with poorly sorted sandy element.</p>								
7.10	o o o o o o o o o o o o			sand and gravel	<p>The gravel chiefly consists of grayish white, angular or subangular, and weathered dacitic tuff which is less than 4cms in diameter.</p> <p>The matrix is the almost same elements of upper bed.</p>							
9.70	o o	Pleistocene middle terrace deposits	sandy clay	<p>This layer is composed of dark grayish brown sandy clay with gravel.</p> <p>The gravel consists of rounded or subrounded dacite and andesite which is 0.5 to 2cms in the mean diameter and 8cms at the largest size.</p>								
12.00	o o										0.40	0.40

Fig. 5-2-5 Boring Log (17)

Depth (m)	Drilling Log	Formation	Lithology	Description	Core Shape					Water Flow (cm/sec)		Water Level Lost Circulation				
					4-20 cm	10-20 cm	5-10 cm	2mm	5cm	2.5 cm	Dry Season		Rainy Season			
12.00			sandy clay	This is the same layer above mentioned.							0.40	0.40	(8/5) (8/19)			
12.60		Pleistocene middle terrace deposits	gravbl	The gravel mainly consists of rounded dacitic and andesitic rocks which is 3 to 4cms in the mean diameter and 23cms at the largest size. The matrix is composed of dark brown, silty and fine-grained sand.							0.40	0.51	(7/24)			
														0.63	0.40	
														0.40	0.40	
														0.40	1.11	
														0.40	0.40	
														0.40	0.51	
				15.80~17.75m This layer is characterized by subround or subangular gravels of light gray to pale reddish gray dacitic tuff.							0.40	0.63				
17.75		Tobe pyroclastic rocks	tuff breccia	The tuff breccia is andesitic and contain abundantly angular fragments of andesite and slate which is 0.5 to 1cm in diameter. 17.75~23.00m This layer has undergone hydrothermal alteration and pyrite occurs as cubes.							0.40	0.40	2.76			
														0.40	0.40	
														0.40	4.06	
														0.40	0.40	
														0.40	3.12	
														0.40	0.51	
														0.40	0.40	
														0.40	0.40	
														0.40	0.40	
														0.40	0.40	
24.00				23.00~24.20m A numerous of calcite veins occur in the dark greenish gray andesitic tuff breccia.							0.40	0.40				

Fig. 5-2-5 Boring Log (18)

Depth (m)	Drilling Log	Formation	Lithology	Description	Core Shape					WaterFlow (cm/sec)		Water Level Lost Circulation	
					<20 cm	10-20cm	5-10cm	2mm - 5cm	> 2 mm	Dry Season	Rainy Season		
24.00	△ △	Toba pyroclastic rocks	tuff breccia	This is the same layer above mentioned.							0.40	(8/5)	
	△			24.20~25.50m This part shows grayish white by alteration.							0.40	(7/24)	
	△ △										0.40		
	△				25.50~29.50m A lot of calcite veins have occurred in greenish gray andesitic tuff breccia.							0.40	
	△ △											0.40	
	△				26.50~29.50m This part includes many angular gravels of andesite and many pyroxene grains more than upper part.							0.40	
	△ △											0.40	
	△ △				27.50m Shear joint; dip angle 40°. Striation has developed on the joint surface.							0.40	
	△ △											0.40	
	△ △				27.60m Shear joint; dip angle 45°. Striation has developed.							0.40	
	△									0.40			
	△ △		28.00~29.50m Shear joint; dip angles 45° and 80°. Striation and slickenside have occurred on the joint surface.							0.40			
	△									0.40			
	△ △		29.50~30.00m This part is composed of black fault breccia which is less than 5cms in diameter and sandy element. Striation and slickenside have occurred.							0.40			
29.50	△	Fault	fault breccia										
30.00	△												

Fig. 5-2-5 Boring Log (19)

Depth (m)	Drilling Log	Formation	Lithology	Description	Core Shape					Water Flow (cm/sec)		Water Level Lost Circulation			
					<20 cm	10-20cm	5-10cm	2mm-5mm	<2 mm	Dry Season	Rainy Season				
0.00		Surface soil	gravelly sand	<p>The gravel mainly consists of angular or subangular acidic tuff and andesitic tuff breccia which is 0.2 to 1cm in diameter.</p> <p>The matrix is composed of pale purplish gray coarse to very coarse-grained sand.</p>											
2.70						gravel	<p>The gravel chiefly consists of rounded or subrounded acidic tuff, tuff breccia, andesite, dacite and granodiorite which is 15 to 20cms in the mean diameter and 48cms at the largest size.</p> <p>The matrix is the almost same elements of upper bed.</p>								
														4.47 m	
															(3/15) pH 8.64
															(7/24) (7/30) (8/5) (8/19)
												0.51			
															0.40 0.40 0.40 0.40
															0.51 0.51 0.40 0.40
												1.28			
															0.63 1.11 0.40 0.51
												1.16			
												1.22 0.87 0.40 0.51			
									0.69						
9.50			sand	This layer is composed of loose medium to coarse-grained sand.								1.11 0.87 0.40 0.40			
10.00			gravel	This part is the almost same gravel of upper part.									1.11 0.40 0.40 0.40		
												0.75 0.40 0.40 0.40			
12.00												0.40			

Fig. 5-2-5 Boring Log (20)

Depth (m)	Drilling Log	Formation	Lithology	Description	Core Shape					Water Flow (cm/sec)		Water Level Lost Circulation
					4-20 cm	10-200 cm	5-10 cm	2 mm 5 cm	2 mm A	Dry Season	Rainy Season	
12.00	0 0		gravel	This is the same layer above mentioned.								
12.20				The slate is black. The lamina and joints have developed in it. Dip angle of lamina is about 5°.							0.40	(7/24)
											0.40	(7/30)
											0.40	(8/5)
										0.40		(8/19)
		Meta-sediments	slate	13.50m Joint; dip angle 65°, straight. 13.80m Joint; dip angle 45°, straight. Striation and slickenside have occurred on the joint surface.						0.40		
											0.75	
											0.40	
											0.40	
14.30												
											0.87	
											0.40	

Fig. 5-2-5 Boring Log (21)

Depth (m)	Drilling Log	Formation	Lithology	Description	Core Shape					Water Flow (cm/sec)		Water Level Lost Circulation
					2-20 cm	10-20 cm	5-10 cm	2 mm - 5 mm	2 mm A	Dry Season	Rainy Season	
0.00		Surface soil	silty sand	This layer consists of dark reddish brown, silty and very fine-grained sand with gravel. The gravel is composed of angular or sub-angular acidic tuff and andesitic tuff breccia which is 0.3 to 1cm in the mean diameter and 5cms at the largest size.								
1.25			gravelly sand	The gravel consists of subangular or subrounded acidic tuff and andesitic tuff breccia which is 0.2 to 0.3cm in the mean diameter. The matrix is composed of pale yellowish gray, silty coarse-grained sand.								
2.45		Pleistocene middle terrace deposits		gravel	The gravel chiefly consists of rounded or subrounded acidic tuff and andesitic tuff breccia which is 2 to 3cms in diameter and 10cms at the largest size. The matrix is composed of pale greenish gray medium-grained sand.							
												0.40 (7/25)
												0.40 (8/19)
												0.40 (8/6)
												0.40
9.70											0.40	
10.00		Toba pyroclastic rocks	tuff breccia	The tuff breccia is characterized by angular fragments of pale green tuff, which is 0.2 to 1cm in diameter. dip angle of bedding; 30°~50° Many joints have developed irregularly at intervals of 2 to 5cms in this bed. Joint surface is covered with dark reddish brown limonite skin. dip angle of joint; 30°, 40° and 65°								0.75 0.40 0.40
12.00												0.40 0.40

Fig. 5-2-5 Boring Log (22)

Depth (m)	Drilling Log	Formation	Lithology	Description	Core Shape					Water Flow (cm/sec)		Water Level Lost Circulation				
					<20 cm	10-20cm	5-10cm	2mm - 5mm	> 2 mm	Dry Season	Rainy Season					
0.00		Surface soil	silty sand	This layer consists of dark reddish brown, silty and very fine-grained sand with gravel. The gravel is composed of rounded tuff which is 1 to 2cm in diameter.												
0.75			sandy silt	This layer consists of pale greenish gray to light gray sandy silt with gravel. The gravel is mainly composed of pale yellow, rounded and fragile tuff which is 0.2 to 0.3cm in the mean diameter.												
			silty sand	This layer consists of pale greenish gray, silty and very fine-grained sand with gravel. The gravel is composed of rounded tuff which is 0.2 to 0.4cms in the mean diameter.												
3.00		Pleistocene middle terrace deposits	gravel	<p>The gravel consists of rounded or subrounded tuff (welded tuff), andesite, granodiorite and slate which is 3 to 5cm in the mean diameter and 27cms at the largest size.</p> <p>The matrix is the almost same element of upper bed.</p>												
12.00																

7.14m
 ∇
 (3 / 15)
 pH 7.94
 (8 / 6)
 (7 / 25)
 (8 / 19)

Fig. 5-2-5 Boring Log (23)

Depth (m)	Drilling Log	Formation	Lithology	Description	Core Shape					Water Flow (cm/sec)		Water Level Lost Circulation
					<20 cm	10-20cm	5-10cm	2mm - 5cm	> 2 mm	Dry Season	Rainy Season	
12.00	○ ○ ○ ○ ○ ○	Pleistocene middle terrace deposits	gravel	This is the same layer above mentioned.								
13.00	△ △ △ △ △ △	Toba pyroclastic rocks	tuff breccia	The tuff breccia is reddish brown and andesitic.								
14.00	△											

Fig. 5-2-5 Boring Log (24)

Depth (m)	Drilling Log	Formation	Lithology	Description	Core Shape					Water Flow (cm/sec)		Water Level Lost Circulation		
					<20mm	10-20mm	5-10mm	2mm - 5mm	> 2 mm	Dry Season	Rainy Season			
0.00		Talus deposits	gravelly sand	<p>The gravel consists of angular or subangular acidic rocks.</p> <p>The matrix is composed of pale yellowish brown, unconsolidated and silty sand.</p>										
3.00			sandy clay	<p>This layer consists of dark gray sandy clay with gravel.</p> <p>The gravel is composed chiefly of rounded or subrounded dacite and andesite, which is 0.5 to 1cm in the mean diameter and 3cms at the largest size.</p>										
4.80		Pleistocene middle terrace deposits	gravel	<p>The gravel consists of rounded or subrounded dacite, andesite and granodiorite which is 3 to 4cms in the mean diameter and 195cms at the largest size.</p> <p>The matrix is composed of yellowish brown, poorly sorted and silty sand.</p>							0.40	0.40	0.4	
7.20~9.15m				This part is only white to pale pink dacite boulder.							0.40	0.40	0.4	
													0.75	0.40
												0.63	0.40	0.4
												0.99	0.40	0.4
12.00														1.22

Fig. 5-2-5 Boring Log (25)

Depth (m)	Drilling Log	Formation	Lithology	Description	Core Shape					Water Flow (cm/sec)		Water Level Lost Circulation
					<20 cm	10-20cm	5-10cm	2mm - 5cm	> 2 mm	Dry Season	Rainy Season	
12.00	○ ○	Pleistocene middle terrace deposits	gravel	This is the same layer above mentioned.								
12.60	△ △		Toba pyroclastic rocks	tuff breccia	The tuff breccia is dark greenish gray, andesitic and hard. A numerous of joints have developed in the bed and pyrite has occurred as cubes along joint surface.						0.87 0.40 0.4	(7/24) (8/5) (8/19)
	△ △	13.90m Shear joint; dip angle 40°. Striation have occurred on the joint surface.										
	△ △	14.40m Shear joint; dip angle 40°										
14.50	△											

Fig. 5-2-5 Boring Log (26)

Depth (m)	Drilling Log	Formation	Lithology	Description	Core Shape					Water Flow (cm/sec)		Water Level Lost Circulation		
					4-20 cm	10-20 cm	5-10 cm	2mm - 5cm	2 mm A	Dry Season	Rainy Season			
0.00		Surface soil	sandy silt	This layer consists of gray and sandy silt. It's accompanied with many roots of plant and charcoal fragments.										
0.30		Talus deposits	sandy silt	This layer is composed of pale brown, poorly sorted and sandy silt with gravel. The gravel mainly consists of pale brown, angular or subangular tuff which is 1 to 5cms in the mean diameter and strongly weathered.										
6.50		Pleistocene middle terrace deposits	sand and gravel	The gravel chiefly consists of subangular or subrounded tuff and welded tuff which is 3cms at the largest size. The matrix is made up of pale purplish brown and crayey sand.										
7.50		Toba pyroclastic rocks	lapilli tuff	The lapilli tuff is acidic and contain abundantly angular fragments of tuff breccia, welded tuff and andesite which is 0.1 to 10cms in diameter, and partly, some calcite veins has occurred in it.										

Fig. 5-2-5 Boring Log (27)

Depth (m)	Drilling Log	Formation	Lithology	Description	Core Shape					Water Flow (cm/sec)		Water Level Lost Circulation		
					4-20 cm	10-20cm	5-10cm	2mm ~ 5cm	> 2 mm	Dry Season	Rainy Season			
12.00	△	Toba pyroclastic rocks	tuff breccia	This is the same rock above mentioned. 12.40m Bedding; dip angle 40°.							0.40 (8/5)			
	△ △									0.40 (8/6) 0.40 (8/19)				
	△ △					13.30m Calcite vein.							0.40	
	△			Fault	fault breccia	This breccia consists of small angular fragments of tuff breccia. Slickenside have occurred on the surface of fragments.							0.40 0.40	
	△												0.40	
	△ △	Toba pyroclastic rocks	tuff breccia											
	△													
	△ △													
	△													
	△ △													
	△													
	△ △					16.50m Calcite vein.								
	△													
	△ △					17.40m Bedding; dip angle 48°.								
	△													
	△ △													
	△													
	△ △													
	△													
	△ △			19.70m Shear joint; dip angle 64°. Striation and slickenside have occurred on the joint surface with clay skin which is 0.2~1mm in thickness.										
20.00	△													
20.20														

Fig. 5-2-5 Boring Log (28)

Depth (m)	Drilling Log	Formation	Lithology	Description	Core Shape					Water Flow (cm/sec)		Water Level Lost Circulation
					<20 cm	10-20cm	5-10cm	2mm - 5cm	> 2 mm	Dry Season	Rainy Season	
0.20		Surface soil	sandy silt	This layer consists of gray and sandy silt. It's accompanied with charcoal fragments.								
		Talus deposits	sandy silt	This sediments is composed of pale reddish brown, poorly sorted and sandy silt with gravel. The gravel mainly consists of subangular or subrounded tuff and welded tuff which is 0.2 to 2cms in diameter.								
3.60		Pleistocene middle terrace deposits	gravel	The gravel consists of subangular or subrounded welded tuff, dacite, andesite and chert which is 3 to 4cms in mean diameter and 34cms at the largest size. The gravel of welded tuff is only in upper part. The matrix is made up of pale brown, well sorted and fine grained sand.								
											0.40	
											0.40	(8/5)
											0.40	(8/6)
											0.40	(8/21)
											0.40	
											0.40	
10.20		Toba pyroclastic rocks	tuff breccia	The tuff breccia is dark gray to dark reddish brown and andesite. It contain angular or subangular fragments of altered andesite which is more than 0.3cms in diameter. Many tensional joints have developed at intervals of 2 to 3cms in this layer. Calcite veins have filled up these joints.							0.40	(8/6)
											0.40	
											0.40	
											0.40	
11.70				11.70m Joint; dip angle 48°.							0.40	

Fig. 5-2-5 Boring Log (29)

Depth (m)	Drilling Log	Formation	Lithology	Description	Core Shape					Water Flow (cm/sec)		Water Level Lost Circulation		
					<20 cm	10-20cm	5-10cm	2mm - 5cm	> 2 mm	Dry Season	Rainy Season			
	△	Toba pyroclastic rocks	tuff breccia	This is the same rock above mentioned.								0.40 (18/21)		
	△ △												0.40	
	△												0.40	
	△ △													
	△													
	△ △													
	△													
	△ △					14.20m Joint; dip angle 42°.								
	△					14.40m Calcite vein has developed more than 1cm in thickness.								
15.00	△ △													

Fig. 5-2-5 Boring Log (30)

Depth (m)	Drilling Log	Formation	Lithology	Description	Core Shape					Water Flow (cm/sec)		Water Level Lost Circulation
					<20 cm	10-20 cm	5-10 cm	2mm - 5cm	> 2 mm	Dry Season	Rainy Season	
				(Standard penetration was performed in this part.)								
4.30		Pleistocene middle terrace deposits	gravel	The gravel consists of rounded or subrounded tuff, tuff breccia, andesite and granodiorite which is 1 to 3cms in the mean diameter and 50cms at the largest size.								
10.50												

Fig. 5-2-5 Boring Log (31)

Depth (m)	Drilling Log	Formation	Lithology	Description	Core Shape					Water Flow (cm/sec)		Water Level Lost Circulation
					<20 cm	10-20cm	5-10cm	2mm - 5cm	> 2 mm	Dry Season	Rainy Season	
				(Standard penetration was performed in this part.)								
10.30		Pleistocene middle terrace deposits	gravel	The gravel consists of rounded or subrounded welded tuff, dacite and andesite which is 2 to 3cms in the mean diameter and 11cms at the largest size.								

Fig. 5-2-5 Boring Log (32)

Depth (m)	Drilling Log	Formation	Lithology	Description	Core Shape					Water Flow (cm/sec)		Water Level Lost Circulation
					<20 cm	10-20cm	5-10cm	2mm	1-5mm	>2 mm	Dry Season	
12.40	○ ○ 	Pleistocene middle terrace deposits	gravel	This is the same layer above mentioned.								
		Intrusive acidic rocks	dacite	The dacite is white and altered. It's characterized by phenocrysts of quartz ranging in 1 to 2mms. Partly, pyrite has occurred in this layer.								
14.60												

Fig. 5-2-5 Boring Log (33)

Depth (m)	Drilling Log	Formation	Lithology	Description	Core Shape					Water Flow (cm/sec)		Water Level Lost Circulation			
					<20 cm	10-20 cm	5-10 cm	2-5 cm	> 2 mm	Dry Season	Rainy Season				
	○	Surface soil	gravelly sand	This layer consists of dark yellowish brown and sandy silt with gravel. The gravel is composed of angular and weathered tuff which is 0.2 to 1cm in the mean diameter.											
1.60	○	River deposits	gravel	The gravel mainly consists of rounded or subrounded tuff breccia, andesite and sandstone which is 1 to 2cms in the mean diameter and 5cms at the largest size. 1.60~1.80m The matrix is yellowish gray and very fine grained sand. 1.80~2.10m The matrix is reddish brown clay. 2.10~10.00m The matrix is gray, well sorted and fine grained sand.											
1.80	○														
2.10	○														
	○														
	○											0.40 (8/19)			
	○											0.40			
	○											0.40			
	○											0.40			
	○											0.40			
10.00	○														

Fig. 5-2-5 Boring Log (34)

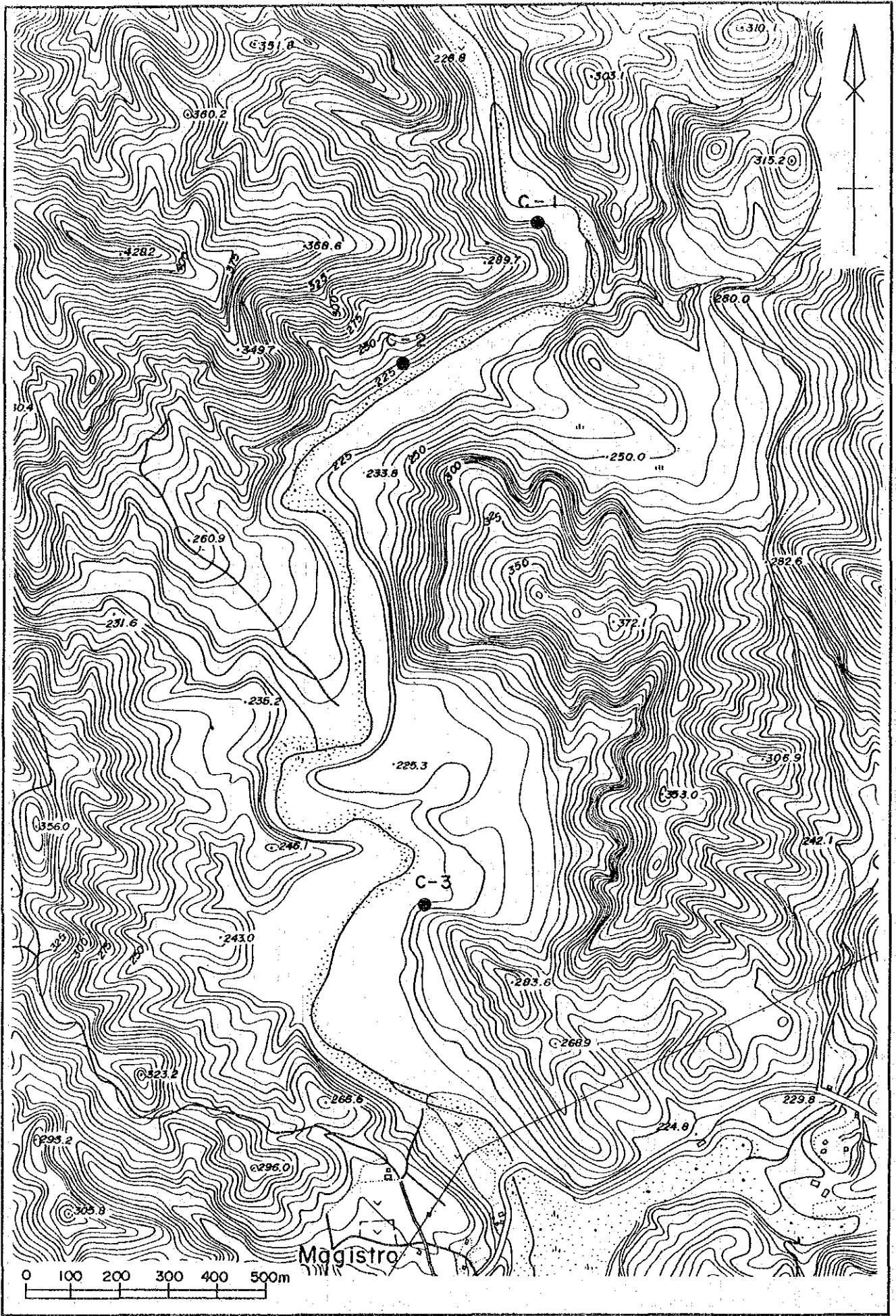


Fig. 5-2-6 Location Map of Fuisse Measuring Site

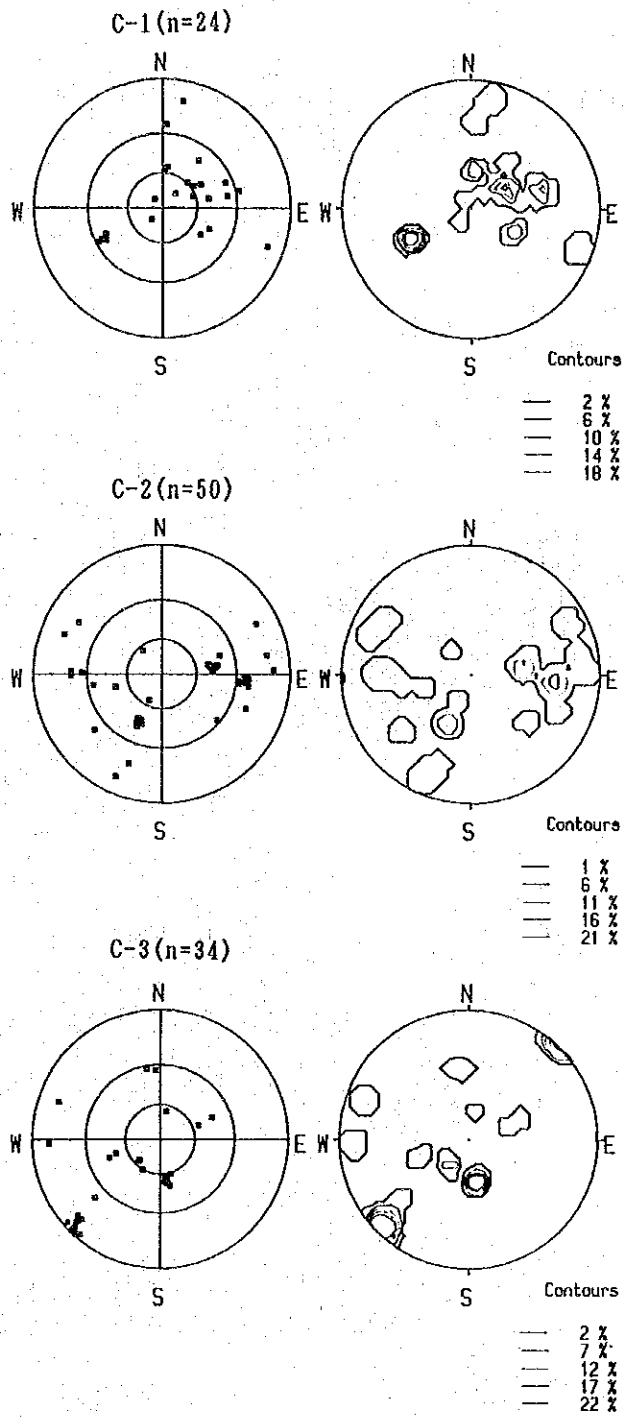


Fig. 5-2-7 Wulff's Net of Fissure Direction

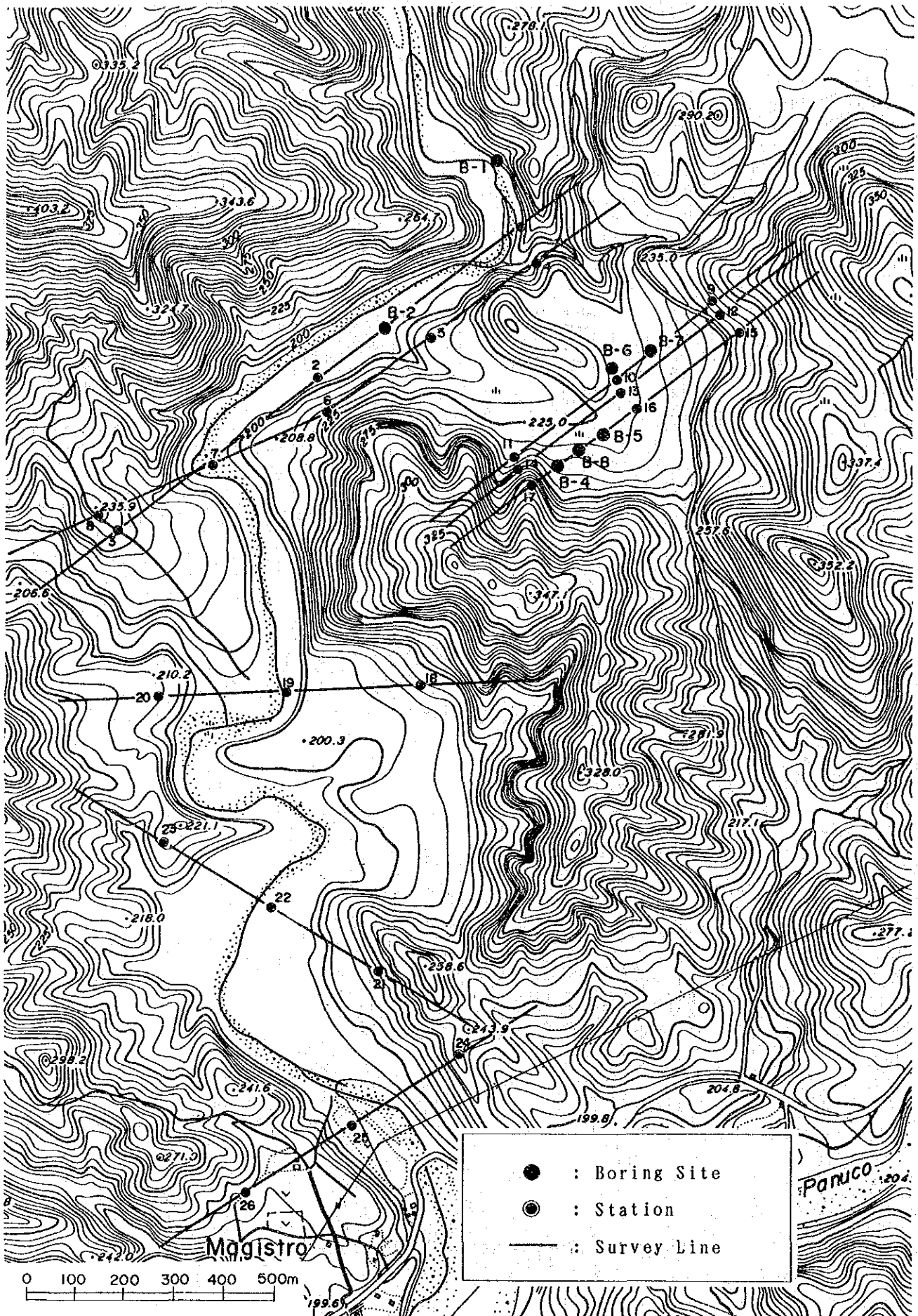


Fig. 5-3-1 Location Map of Electrical Prospecting Station (New El Coco)

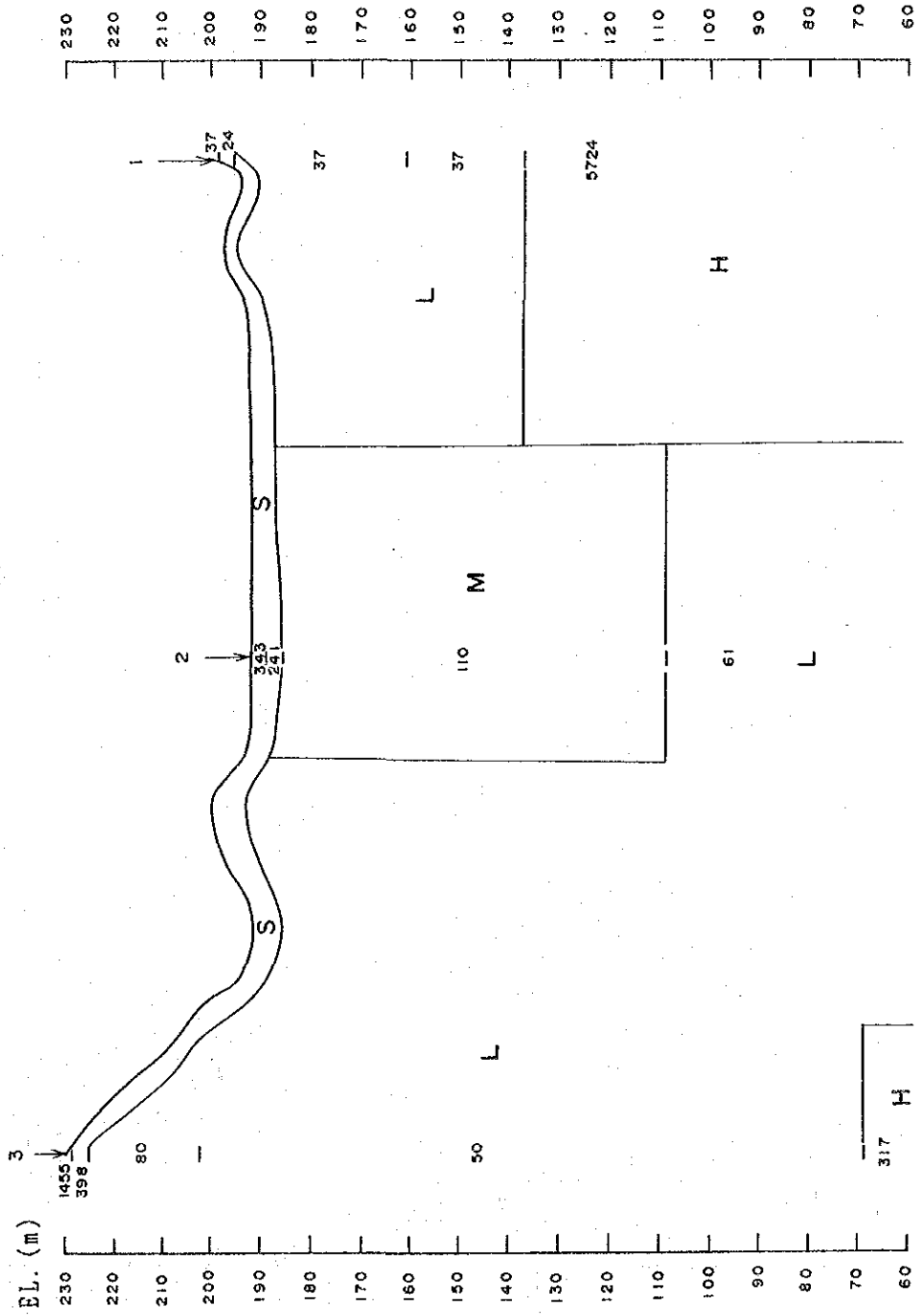


Fig. 5-3-2 Resistivity Cross Section (1)

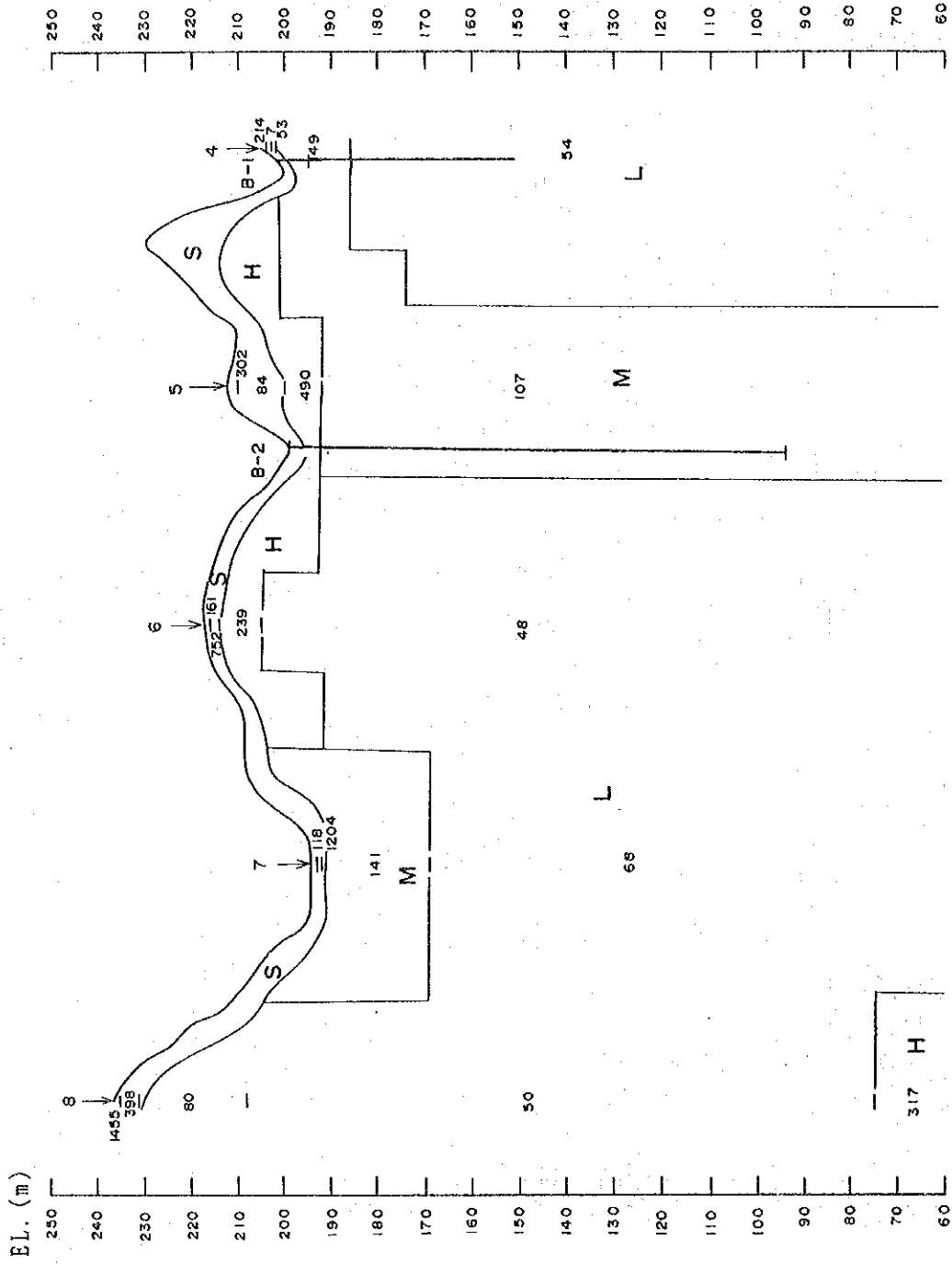


Fig. 5-3-2 Resistivity Cross Section (2)

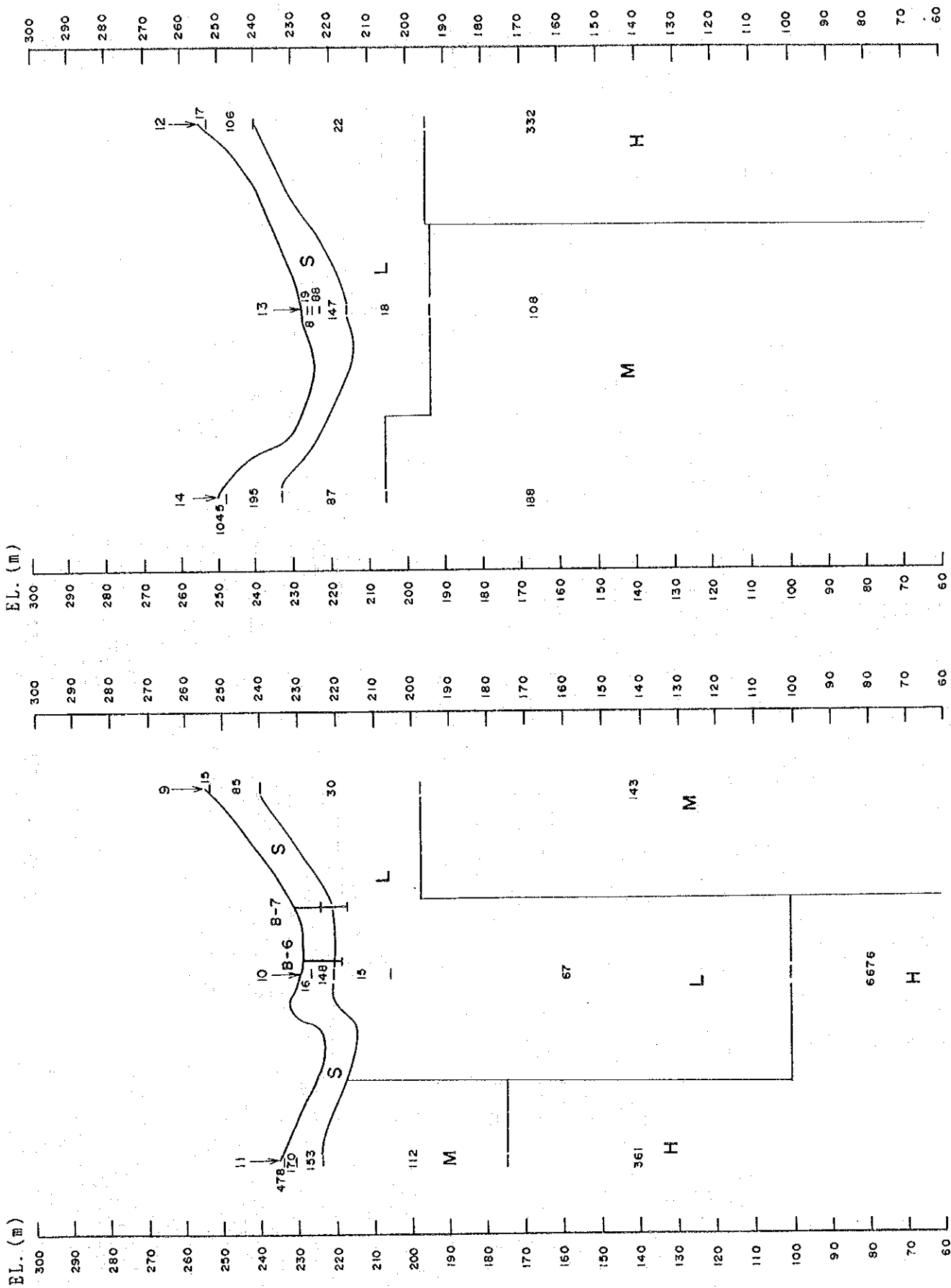


Fig. 5-3-2 Resistivity Cross Section (3)

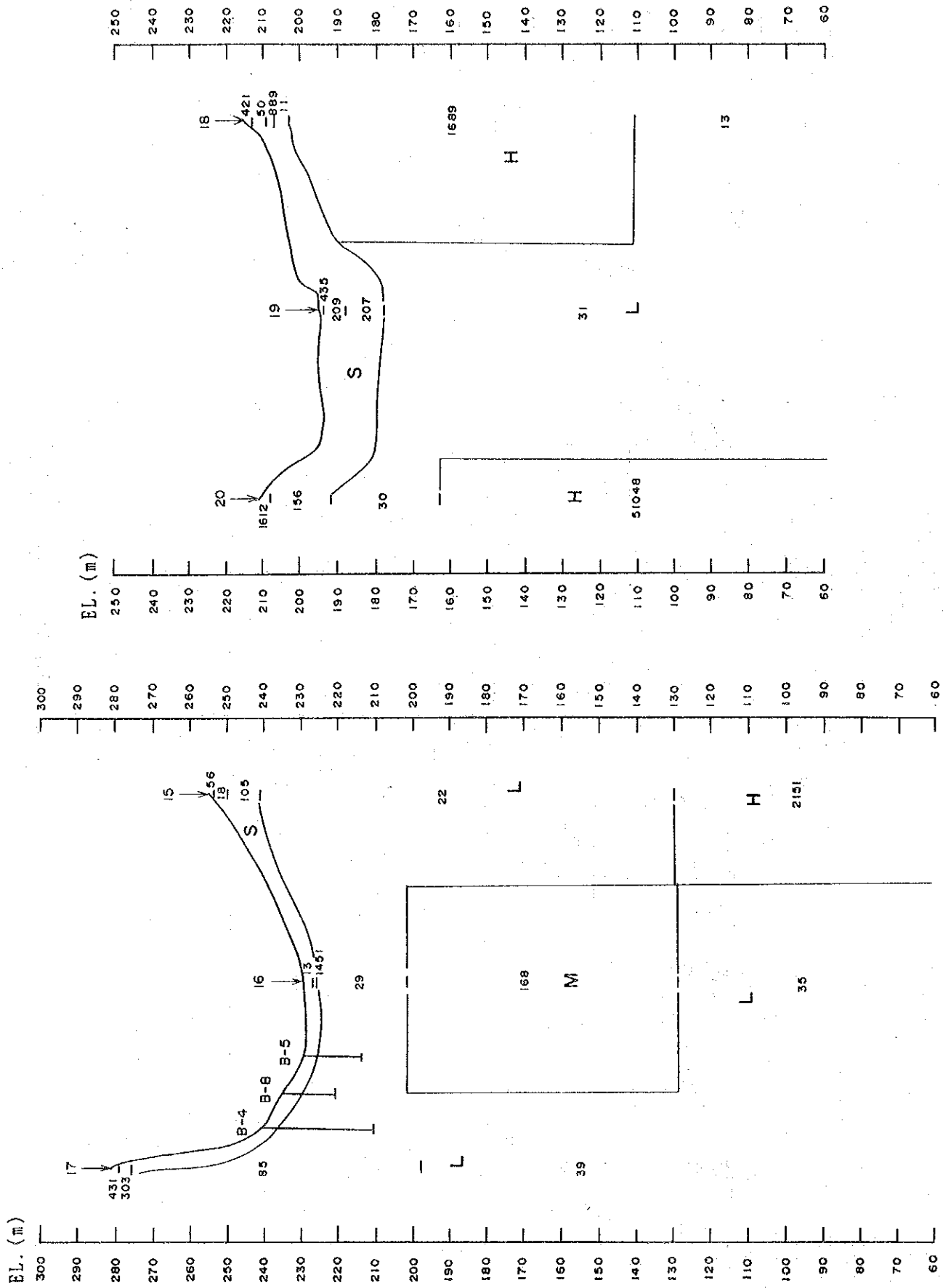


Fig. 5-3-2 Resistivity Cross Section (4)

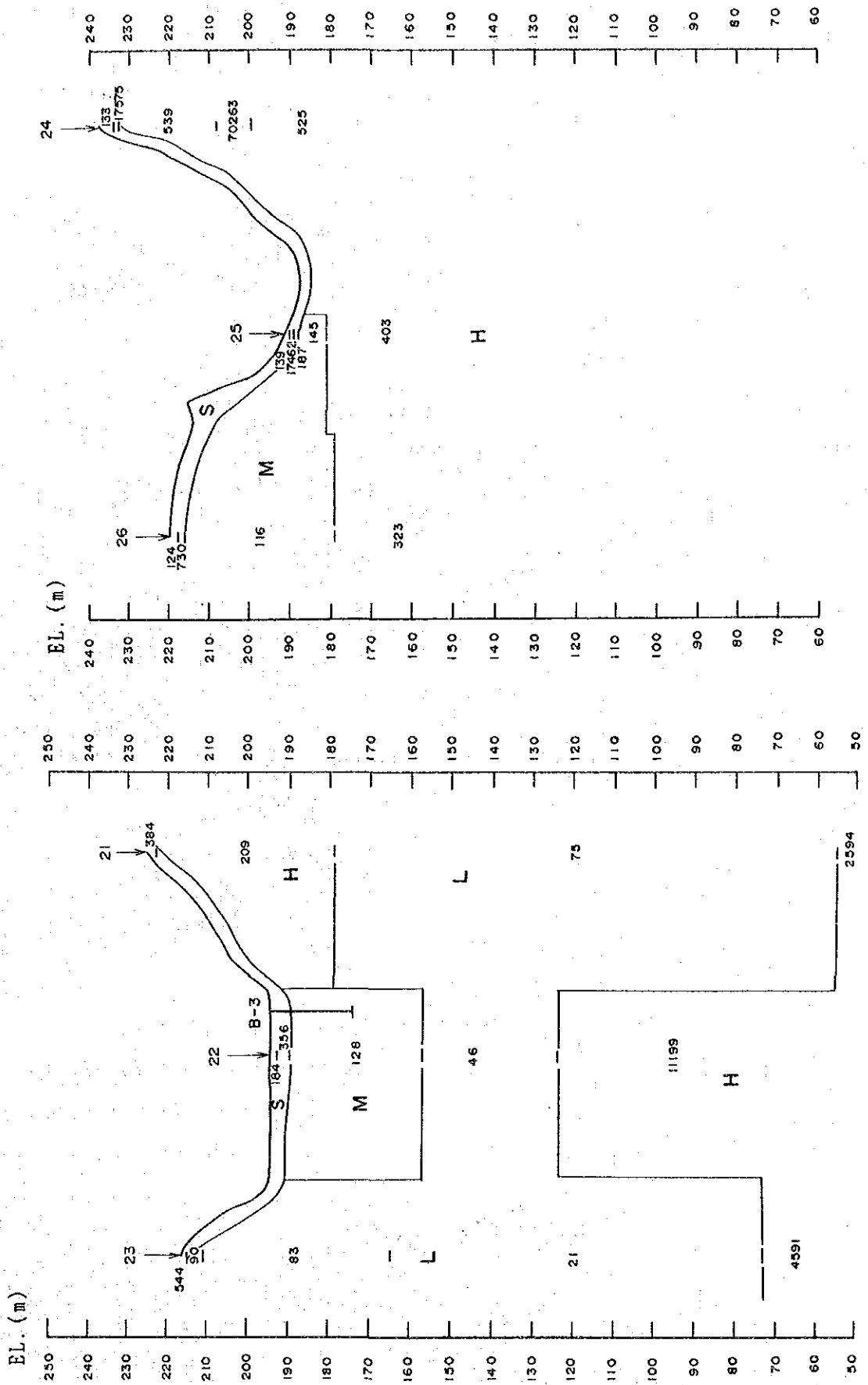


Fig. 5-3-2 Resistivity Cross Section (5)